Linking metal centres with diimido ligands: synthesis, electronic and molecular structure and electrochemistry of organometallic ditungsten complexes [{WCl$_2$(Ph$_2$PMe)$_2$(CO)}$_2$(N–X–N)] (X = π-conjugated organic)

Graeme Hogarth,* David G. Humphrey, Nikolas Kaltsoyannis, Woo-Sung Kim, Mo-yin (Venus) Lee, Tim Norman and Simon P. Redmond

Chemistry Department and Centre for Theoretical and Computational Chemistry, University College London, 20 Gordon Street, London, UK WC1H 0AJ

Tungsten(IV) diimido-bridged complexes [{WCl$_2$(Ph$_2$PMe)$_2$(CO)}$_2$(μ-N–X–N)] have been prepared *via* oxidative addition of diisocyanates to two equivalents of [WCl$_2$(Ph$_2$PMe)$_4$]. *para*-Substituted monoimido complexes [WCl$_2$(Ph$_2$PMe)$_2$(CO)(NC$_6$H$_4$X-*p*)] (X = I, Br or C≡CPh) have also been prepared but attempts to couple the X = I complex as a route to diimido-bridged complexes were unsuccessful. All complexes are air-stable crystalline solids and five diimido (N–X–N = *p*-NC$_6$H$_4$N, *p*-N-*o*-MeC$_6$H$_3$N, *p*-N(*o*-MeOC$_6$H$_3$C$_6$H$_3$OMe-*o*)N, 1,5-NC$_{10}$H$_6$N or *m*-NC$_6$H$_4$N) and one monoimido complex (X = I) have been characterised crystallographically. All show the same gross structural features, namely a *trans* arrangement of phosphines and *cis* chlorides. The central aryl ring generally lies approximately in the Cl$_2$(CO) plane (torsional angles 4.1–26.1°) except for one complex in which the ring lies almost perpendicular to this (torsional angle 80.2°). A series of density functional calculations conducted on model mono- and di-imido tungsten-(VI) and -(V) compounds indicated that the most stable aryl ring orientation is perpendicular to the plane containing the *trans* phosphines, *i.e.* as found in all cases except one (N–X–N = *p*-NC$_6$H$_4$N). The anomaly in the latter may be due to cocrystallisation with chlorobenzene. In order to assess the degree of communication between the tungsten(IV) centres through the highly π-conjugated diimido linkages, electrochemical studies have been carried out. All diimido-bridged complexes show two closely spaced oxidative processes at low temperature indicative of weak electronic communication. The reductive chemistry of the *para*-phenylene bridged complexes is different from other diimido complexes, displaying two closely spaced reductive processes. Spectro-electrochemical studies have also been carried out on N–X–N = *p*-NC$_6$H$_4$N, oxidation at +1.2 V leading to CO loss. In order to gain further insight into the nature of the electronic communication between metal centres density functional calculations were carried out and were generally in agreement with the electrochemical results, suggesting that there is at best a weak interaction between the metal centres in these π-conjugated diimido-bridged complexes.

Introduction

Developing, understanding and exploiting electronic communication between metal centres is a continuing area of interest to both the synthetic and theoretical chemist[1] and since the pioneering days of Creutz and Taube[2] many exciting and novel developments have been made. The focus of most synthetic studies in this area are complexes in which the metals are linked *via* a π-conjugated organic backbone. For example, Gladysz and co-workers[3] and others[4] have shown that when metal centres are linked *via* π-conjugated acetylide based groups a high degree of electronic communication between them can be achieved. Since multiple bonding between metal atoms and main group elements such as carbon and nitrogen is highly delocalised in nature[5] this allows for strong conjugation between the metal and heteroatom, and related studies have focused on the use of metal complexes with multiply bonded ligands such as carbon-based alkylidyne[6] and alkylidene[7] complexes.

The binding of imido ligands to transition metal centres is well known and occurs for metals in a variety of oxidation states, although high-valent centres in which the metal has a d^0–d^2 electronic configuration are particularly stable.[5] Such ligation is particularly desirable for the design of π-conjugated systems since strong interactions occur between the metal d orbitals and p orbitals on nitrogen. This interaction is well developed such that the imido ligand is a strong π-donor moiety.[8] Joining metal centres with imido functionalities linked *via* a conjugated unsaturated organic moiety should allow them to communicate with one another. To date only a few examples of this type of ligation have been reported. Thus, tungsten,[9–11] molybdenum,[12–14] rhenium,[15,16] niobium,[17] vanadium[18] and uranium[19] centres have been linked *via* a *para*-phenylene diimido ligand, however other π-conjugated organic backbones have only been utilised to couple dirhodium centres.[20] We recently reported the facile synthesis of two such phenylene linked tungsten(IV) complexes, namely the isomeric pair [{WCl$_2$(Ph$_2$PMe)$_2$(CO)}$_2$(N–X–N)] (X = *p*-C$_6$H$_4$, or *m*-C$_6$H$_4$).[9] Since such complexes are easily prepared in high yield *via* oxidative addition of diisocyanates to [WCl$_2$(Ph$_2$PMe)$_4$][21,22] we decided to exploit this synthetic procedure in order to prepare a range of such complexes and assess the degree of communication between the metal centres as a function of the π-conjugated organic linking unit. Herein we report the synthesis of a wide range of such complexes together with electrochemical studies and molecular orbital calculations in an attempt to assess and understand the size and nature of the metal–metal interaction. Further, we have attempted to prepare other linked complexes *via* coupling of monoimido fragments. A preliminary account of an aspect of this work has appeared.[9]

Results

During the course of these studies a number of amines **I**, isocyanates **II** and tungsten(IV) imido complexes **1** were utilised.
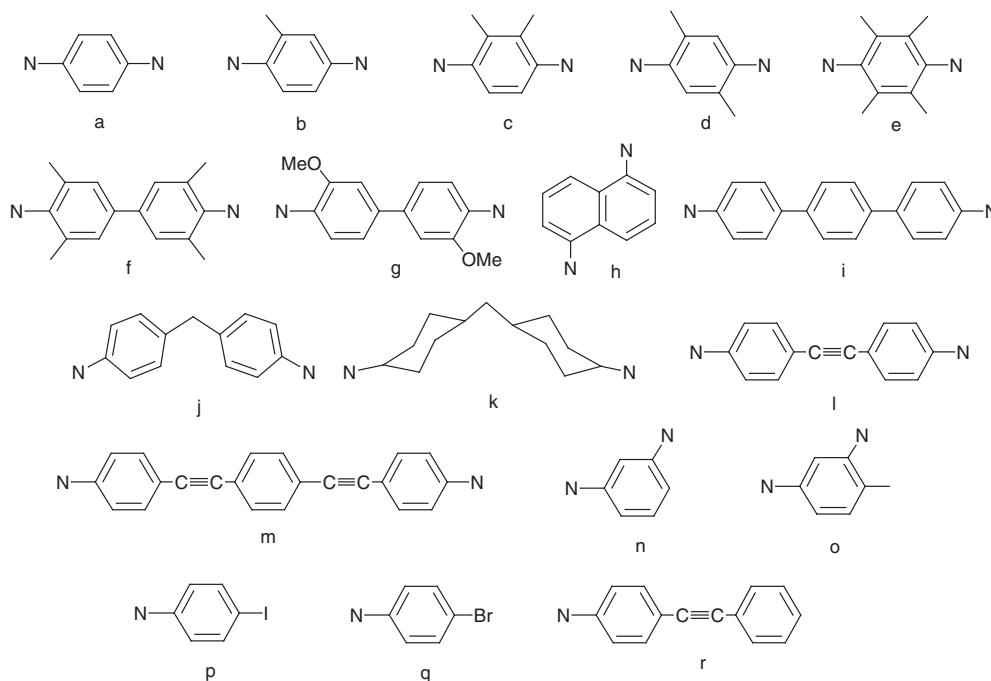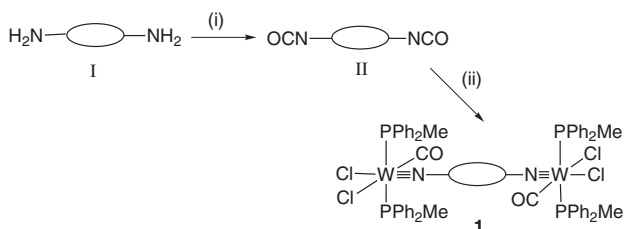
Chart 1

Chart 1

Chart 1 shows the backbones of these (together with the labelling which is used throughout), while Scheme 1 shows the general reaction conditions employed.

Scheme 1 (i) (COCl$_2$)$_3$, 180 °C; (ii) 2[WCl$_2$(Ph$_2$PMe)$_4$], RT, −2Ph$_2$-PMe.

(i) Synthesis of amines and isocyanates

The majority of the amines and diamines used in this study were obtained commercially, however those containing the ethynyl group were prepared (Scheme 2). The alkyne *para*-
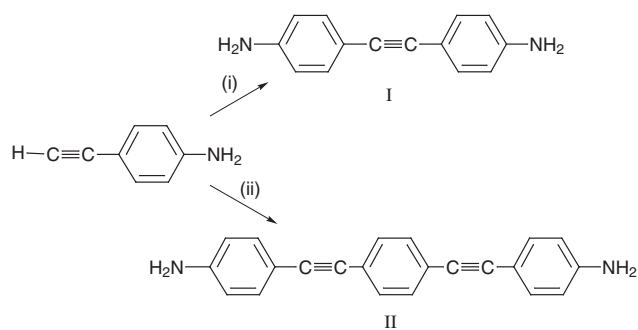
Scheme 2 (i) *para*-Iodoaniline, [PdCl$_2$(PPh$_3$)$_2$]/CuI; (ii) 0.5 *para*-iodobenzene, [PdCl$_2$(PPh$_3$)]/CuI.

ethynylaniline [23] proved to be a pivotal intermediate in the synthesis of diamines **Il** and **Im**. Palladium-catalysed coupling reactions were carried out using the standard literature procedures [24] and gave moderate unoptimised yields (**Il**, 28; **Im**, 55%). Both showed NH stretches in the IR spectrum, while a band at 2206 cm^{-1} of **Im** is assigned to the asymmetric mode of

the ethynyl moieties. As expected, no such absorption was seen for **Il**. *para*-Aminodiphenylethyne **Ir** was prepared in a similar manner upon coupling of *para*-iodoaniline and phenylethyne; conditions being optimised to give a 72% yield.

While a few of the diisocyanates were commercially available, in order to extend the scope of the diimido linkage reaction it proved necessary to prepare a number of new such compounds (Scheme 1). Conversion of the diamines into diisocyanates was achieved using triphosgene (COCl$_2$)$_3$.[25] Yields varied enormously (17–90%), low amounts normally being associated with poor solubility of the diamine and low volatility of the diisocyanate, the latter making purification by sublimation difficult. Most diisocyanates were white solids and all were characterised by bands between 2295 and 2250 cm^{-1} in the IR spectrum associated with the NCO group. With ethynylamines an excess of triethylamine was necessary in order to prevent attack of the released HCl at the carbon–carbon triple bond. *para*-Iodophenyl isocyanate **IIp** could not be prepared from *para*-iodoaniline **Ip** and triphosgene, the former being recovered even under forcing conditions. Use of phosgene in toluene did give **IIp** (55%) being easily purified by sublimation. Halide deactivation of anilines towards phosgene attack and isocyanate formation is not noted in many current texts, despite being made clear in the early literature.[26]

(ii) Synthesis and characterisation of tungsten(IV) imido complexes

Room temperature reaction of 2 equivalents of [WCl$_2$(Ph$_2$-PMe)$_4$] and diisocyanates **II** resulted in the slow formation (2–48 h) of the diimido-bridged tungsten(IV) complexes **1a–1o** in yields of 40–93%, while analogous monoimido complexes **1p–1r** were prepared similarly. Reactions were easily monitored by a progressive change from orange to either green or purple and also by IR spectroscopy, the isocyanate band at around 2200–2150 cm^{-1} disappearing to be replaced by a band assigned to the metal-bound carbonyl at around 1975–1955 cm^{-1}. High molecular weight isocyanates were not very soluble in toluene and these reactions could also be followed by their slow dissolution. Yields were generally quantitative by ^{31}P NMR spectroscopy, with no evidence of other products. Isolation was generally straightforward being achieved by precipitation from the toluene solution (after concentration) and washing with

light petroleum to remove released phosphine. All tungsten imido complexes **1** are stable in air, and recrystallisation upon slow diffusion of methanol into a saturated dichloromethane solution gave green or purple crystalline solids. In a few instances released phosphine proved difficult to remove from the small amounts of tungsten complex formed and satisfactory analytical results could not be obtained.

Characterisation was generally straightforward being based on elemental analysis, IR, ^{1}H and ^{31}P NMR spectroscopy and positive-ion FAB mass spectra. In the IR spectra the metal-bound carbonyl appears as a broad band at 1975–1955 cm^{-1}, confirming the oxidative addition of the isocyanate. All positive-ion FAB spectra showed a peak corresponding to the loss of a single carbonyl group, together with other peaks due to sequential loss of the second carbonyl and the phosphines. The ^{31}P NMR spectra generally consist of a single resonance at around δ 3, indicating the equivalence of all phosphorus atoms, with satellites due to coupling to tungsten (J_{PW} = 290–292 Hz). For asymmetric complexes **1b** and **1o** two phosphorus resonances were observed in both cases, being separated by about 1 ppm. Proton NMR spectra showed complex signals in the aromatic region of the spectrum due to the phenyl groups of the phosphine ligands. Generally, the aryl protons of the imido ligands appeared further upfield of these, but in a few cases it was difficult to deconvolute resonances associated with the arylimido group and the phenyl rings on the phosphines. For example, in the 3,3′-dimethoxybenzidene complex **1g** the arylimido protons appeared between δ 6.57 and 6.53 as two doublets (J 8.4 Hz) and a singlet, while the phenyl protons appeared as a multiplet between δ 7.69 and 7.24. Further, all spectra also showed a triplet at around δ 2.3 assigned to the phosphorus-bound methyl group. All ^{13}C NMR spectra showed a low-field triplet at around δ 242 assigned to the carbonyl ligand, a complex set of peaks between δ 155 and 105 due to aromatics and a triplet at around δ 13 assigned to the methyl groups of the phosphines.

Reaction of compound **IIa** with one equivalent of [WCl$_2$(Ph$_2$PMe)$_4$] resulted only in the formation of **1a** and unchanged tungsten(II) complex with no evidence for an intermediate mononuclear complex, the latter being the case in all other reactions except one. This exception was the reaction with 1,5-diisocyanatonaphthalene **IIh**. Here, long reaction times were needed as the isocyanate was only sparingly soluble in toluene. Monitoring the reaction by IR spectroscopy showed the expected decrease in intensity of the isocyanate stretch (2270 cm^{-1}), together with the anticipated growth of the new metal–carbonyl absorption (1964 cm^{-1}). However, a further absorption at 2094 cm^{-1} also grew in concomitant with that of the tungsten carbonyl which latter decreased in intensity. In an attempt to isolate this intermediate, addition of a 1:1 ratio of reactants was carried out but again only **1h** (albeit in lower yields) and [WCl$_2$(Ph$_2$PMe)$_4$] were isolated after work-up.

In a second approach towards the synthesis of tungsten bridged diimido complexes, we attempted to prepare a biphenyl diimido complex *via* the Ullman coupling[27,28] of the mononuclear iodo-complex **1p**. Dissolution of **1p** in dimethylformamide followed by treatment with activated copper at high temperature resulted in the formation of a dark solution from which a brown intractable oil was isolated after removal of precipitated copper iodide. Proton NMR spectroscopy indicated the presence of some unchanged **1p**, together with other unidentified species, while in the ^{31}P NMR spectrum a number of species were also observed. The mass spectrum showed peaks centred at *m/z* 1565 and 1173 which could be due to a ditungsten complex, but the IR spectrum showed the complete absence of any carbonyl absorptions. Clearly, if coupling is taking place, then it is not clean and other secondary processes are also operating. Repeating the reaction using pyridine as the solvent gave a similar result, although a carbonyl resonance was apparent in the IR spectrum. Here again, however, NMR data

suggested a complex reaction mixture and thus this strategy was not pursued further.

(iii) X-Ray crystallographic studies

Single-crystal X-ray crystallographic studies were carried out on six of the tungsten(IV) complexes, namely diimido-bridged **1a**, **1b**, **1g**, **1h** and **1n**, and mono-imido **1p**. All were crystallised upon slow diffusion of methanol into saturated dichloromethane solutions, except **1a** which was crystallised upon slow diffusion of methanol into a saturated chlorobenzene solution. Selected bond lengths and angles for these and related tungsten imido complexes are given in Table 1, while views of the molecules are shown in Figs. 1–6. For both **1g** and **1h** the asymmetric unit contains two half molecules and there are no intermolecular contacts between them. Further, **1a** contains a disordered molecule of chlorobenzene in the asymmetric unit while **1h** contains a molecule of dichloromethane. Again there are no intermolecular contacts. In all cases except for **1g** all non-hydrogen atoms were refined anisotropically. For **1g** a number of atoms were disordered over two sites (50% occupancies) and these and the phenyl rings were refined only isotropically. The representations of the molecules of **1g** shown in Fig. 3 show the average of the disordered sites. In **1b** (Fig. 2) the methyl carbon on the aryl ring, C(5), is disordered over two sites. It is given only a 50% occupancy as the inversion centre generates the second carbon atom. This renders crystallographically equivalent the two non-equivalent tungsten centres in the molecule.

All molecules contain an approximately octahedral tungsten(IV) centre(s), the co-ordination sphere consisting of *trans*-phosphines [P–W–P 166.4 ± 2.7°], *cis*-chlorides [Cl–W–Cl 88.9 ± 2.1°] and a *cis* arrangement of imido and carbonyl ligands [N–W–C 89.9 ± 2.9°]. Tungsten–phosphorus bonds are within the expected range [W–P 2.529 ± 0.021 Å], while the tungsten–chlorine bond *trans* to the imido [W–Cl 2.462 ± 0.016 Å] is not significantly different to that *trans* to the carbonyl [W–Cl 2.458 ± 0.013 Å], the absence of a *trans* influence at the tungsten(IV) centre being expected.[29] The tungsten–carbon bond to the carbonyl is as expected [1.144 ± 0.014 Å] and the W–C–O vector is essentially linear. Since most of the molecules contain an inversion centre, then the carbonyls on different tungsten centres are constrained to lie on opposite sides of the molecule. This is not the case with *meta* complex **1n**, the asymmetric unit containing a full molecule with carbonyls lying on the same side of the molecule. The short tungsten–nitrogen distance [W–N 1.755 ± 0.012 Å] is within the range expected from studies on other tungsten imido complexes[5,8] and the near linearity at nitrogen [W–N–C 171.1 ± 2.2°] suggests that it is acting as a 4-electron donor to the tungsten centre.

The most striking feature of these structures is the relative orientation of the aryl ring(s) of the imido ligands to the tungsten centre as illustrated in Figs. 1–6. This is represented in Table 1 by a torsion angle, which is that between the plane of the aryl ring(s) and the WCl$_2$(CO) plane, ranging between 4.1° in **1p** to 80.2° in **1a**. Thus, in the latter the phenylene ring lies approximately perpendicular to this plane lying almost parallel to the WP$_2$(CO) plane. This situation is, however, the only one of its type. Thus, for all other diimido-bridged molecules torsion angles vary between 5.8 and 26.1°, that is the aryl ring(s) lie approximately in the WCl$_2$(CO) plane. It is noteworthy that there are no intermediate values *i.e.* 35–75°, that is the aryl ring(s) either lie close to one plane or the other. The two independent molecules in the asymmetric units of **1g** and **1h** vary by virtue of the different torsional angles they adopt; **1g** (A, 26.1; B, 17.3°) and **1h** (A, 10.7; B, 6.2°). Otherwise these independent molecules of **1g** and **1h** are very similar, minor differences being the carbonyl C–O distances in **1g** [1.139(13) and 1.153(13) Å] and nitrogen–carbon [1.44(2) and 1.41(2) Å] and tungsten–nitrogen [1.746(11) and 1.757(13) Å] in **1h**.
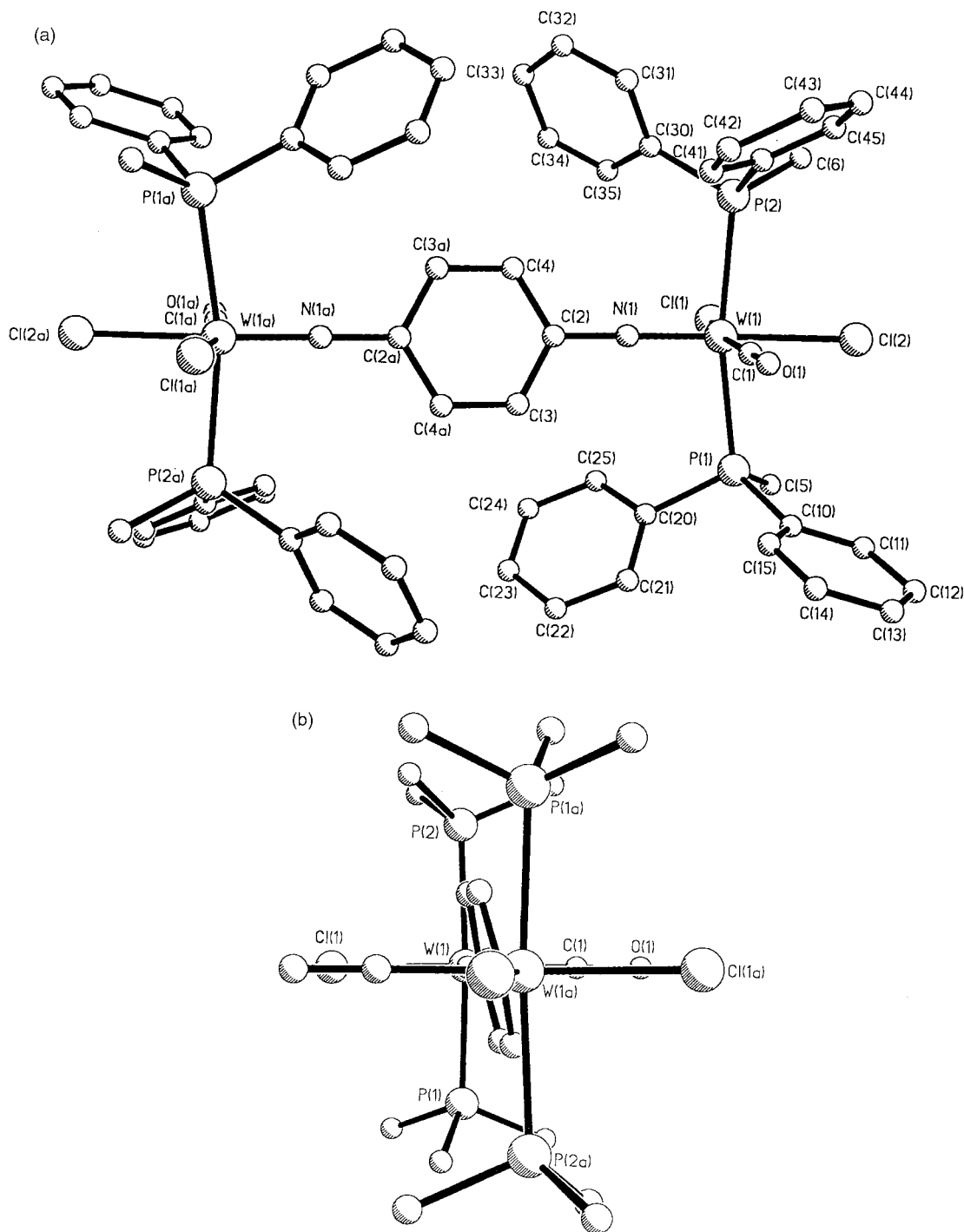
Fig. 1 Molecular structure of complex **1a**; (a) full molecule, (b) end-on (phenyl rings omitted for clarity).

Further, a number of the bond angles around tungsten vary in **1h**, representative examples being the Cl–W–Cl [90.9(2) and 86.7(2)°] and P–W–P [163.65(12) and 169.12(13)°] angles. Generally, however, little conformational change is required about the tungsten centre for the diimido-linkage to take up different conformations.

While differences in individual bond lengths and angles within isomeric **1a** and **1n** are not significant, the gross structures are quite different. In *para*-**1a** the tungsten centres, related by the crystallographic inversion centre, are necessarily eclipsed; in *meta*-**1n** each metal centre is crystallographically unique being twisted by approximately 7.4° with respect to one another. It is probable that this arises to reduce adverse steric interactions between the phenyl rings of the phosphine ligands on adjacent metal centres, being minimised by the twist. Thus, the central aryl ring makes torsional angles of 5.8 and 23.9 to the

W(1)Cl$_2$(CO) and W(2)Cl$_2$(CO) planes respectively. Such a twist renders the two metal centres crystallographically in-equivalent. However, in solution they are equivalent suggesting that the energy barrier to this twist about the W–N bonds is small. Again, it should be noted that this has little effect on the conformation at the metal centre with maximum differences in bond angles and lengths at the two independent tungsten centres being within the 3σ range, that is not significant.

The mononuclear *para*-iodoimido complex **1p** (Fig. 6) is closely related to the *para*-tolyl complex [WCl$_2$(Ph$_2$PMe)$_2$(CO)-(NC$_6$H$_4$Me-*p*)] **1t** structurally characterised by Mayer and co-workers [22a] (Table 1). Again, there are only small differences between these two molecules which are characterised by torsion angles of 4.1 (**1p**, X = I) and 4.3° (X = Me), and suggesting that exchange of electron-releasing and electron-withdrawing
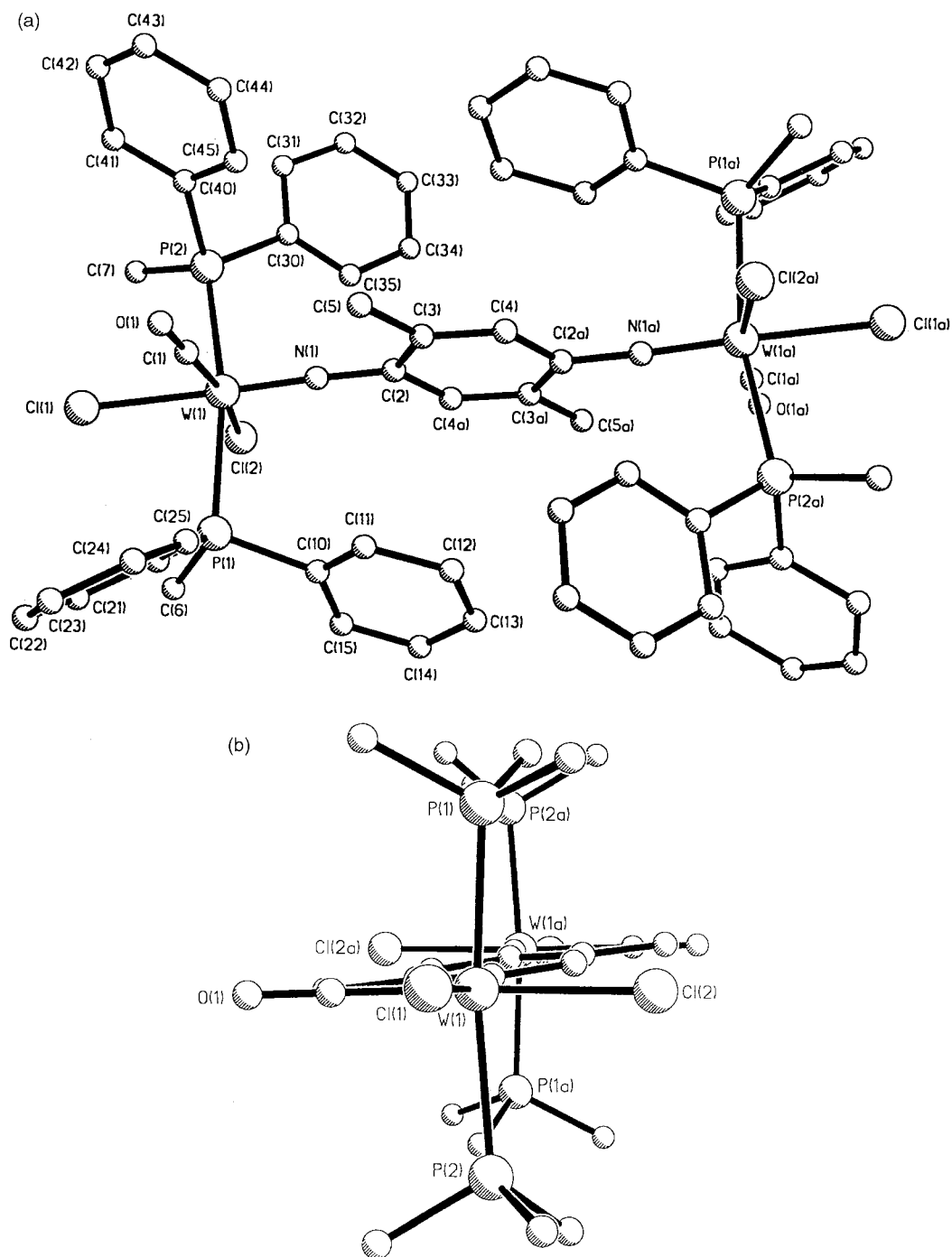
Fig. 2 Molecular structure of complex **1b** as in Fig. 1. Showing the Me group of the central ring disordered over two sites, C(5) and C(5a).

groups at the *para* position has little effect upon the binding of the imido ligand or the tungsten centre in general.

(vi) Electronic structure calculations: central ring rotation

As discussed above, a striking feature of the crystal structures of complexes **1a**, **1b**, **1g**, **1h**, **1n** and **1p** is the relative orientation of the aryl ring(s) of the imido ligands and the tungsten centre. In **1a** the aryl ring is almost coplanar with the two phosphorus atoms and the tungsten centre, in contrast to other compounds in which the ring is rotated by virtually 90° to this plane. Further, this ring orientation is also found in [WCl$_2$(Ph$_2$PMe)$_2$-(CO)(NC$_6$H$_4$Me-*p*)] **1t**[22a] and the tungsten(v) diimido-bridged complex [{WCl$_3$(PMe$_2$Ph)$_2$}$_2$(μ-*p*-NC$_6$H$_4$N)] **2**.[11] In order to establish if there is an electronic explanation for the atypical geometry of **1a**, we have conducted a series of density functional calculations on the model compounds [WCl$_2$(PH$_3$)$_2$-(CO)(NPh)] **1s′**, [WCl$_3$(PH$_3$)$_2$(NPh)] **3′**, [{WCl$_2$(PH$_3$)$_2$(CO)}$_2$-(μ-*p*-NC$_6$H$_4$)] **1a′** and [{WCl$_3$(PH$_3$)$_2$}$_2$(μ-*p*-NC$_6$H$_4$)] **2′**, in which the substituted phosphine ligands of the actual compounds are replaced by PH$_3$ groups. X-Ray crystallography has shown that in the unsubstituted phosphine analogues of both of the mononuclear systems **3′** and **1s′** and the dinuclear compound **2′** the aryl ring lies close to the Cl$_3$/Cl$_2$(CO) plane.[11,22,30]

The calculations reveal the anticipated electronic structures, with a single electron in the M–Cl π antibonding highest occupied molecular orbital (HOMO) of the formally tungsten(v) **3′** and two electrons in the equivalent MO of **1s′** (W–Cl antibonding/W–CO back bonding). The ditungsten compounds **2′** and **1a′** have twice the number of metal-based electrons as **3′** and **1s′** respectively. Compound **1a′** is predicted to have no unpaired electrons, while the two metal-based electrons of **2′** give rise to a high spin triplet state 27.5 kJ mol^{-1} more stable than the spin paired singlet.
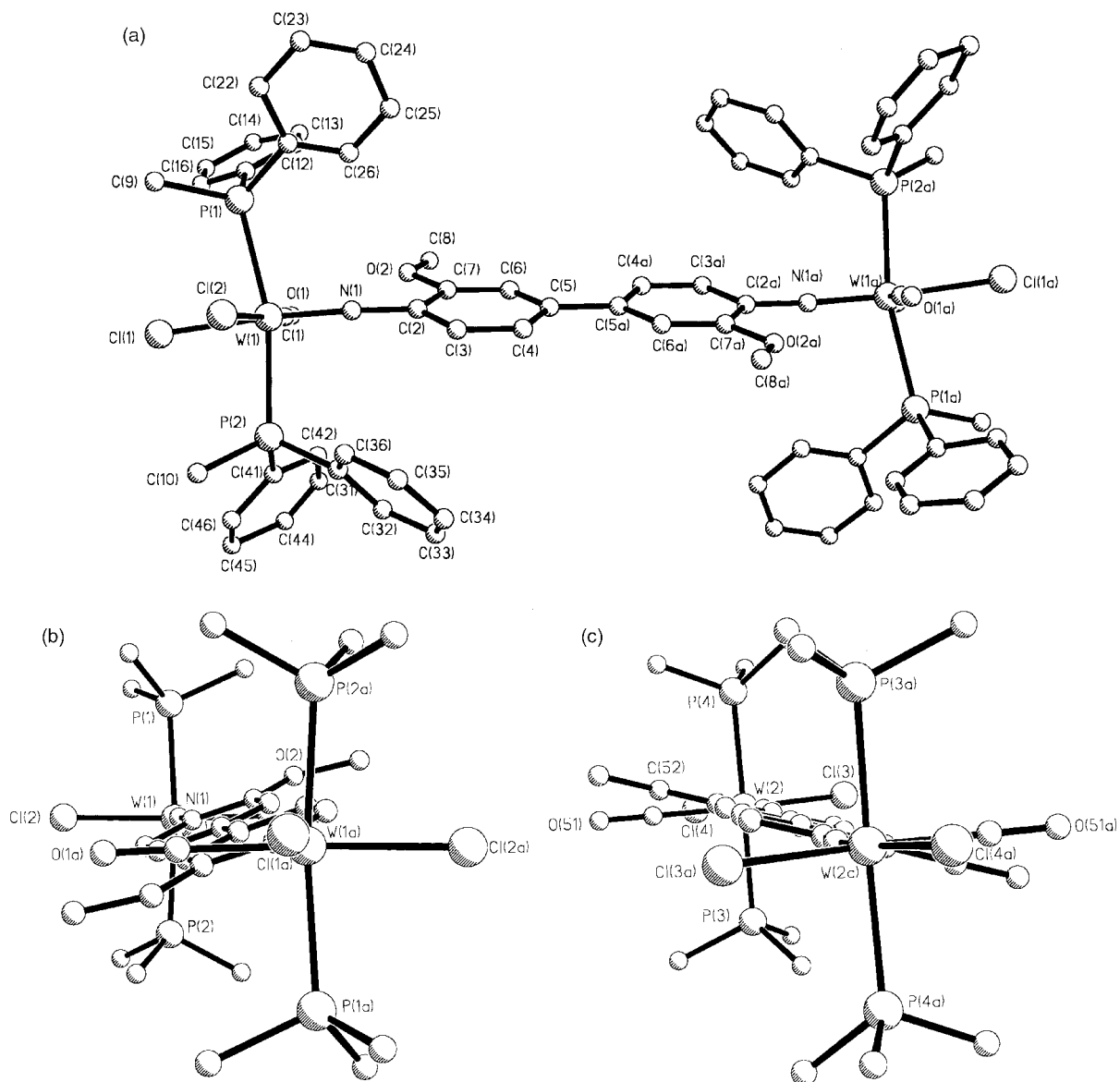
Fig. 3 Molecular structure of complex **1g**; (a) full picture of molecule A, (b) molecule A end-on (phenyl rings omitted for clarity), (c) molecule B end-on (phenyl rings omitted for clarity).

For each of the molecules the aryl ring was rotated from coplanarity with the $Cl_3/Cl_2(CO)$ groups to perpendicular in steps of 10°, and Fig. 7 presents the variation in the total molecular binding energies (kJ mol^{-1}) as this distortion is performed. Our calculations clearly indicate that the most stable orientation of the aryl ring is similar in all four cases, *i.e.* that the preferred geometry has the ring almost coplanar with the $Cl_3/Cl_2(CO)$ groups. This is in agreement with the crystal structures of the substituted phosphine complexes **1s**, **2** and **3**, but contrary to **1a**. We therefore conclude that the orientation of the central aryl ring in **1a** does not have an intramolecular cause, and arises as a result of external effects, probably crystal packing forces. In this respect it is noteworthy that **1a** is co-crystallised with chlorobenzene and it may be the interaction between the cocrystallised molecules which leads to **1a** adopting an unfavourable central ring geometry. The relatively small energy differences between the least stable (80–90° ring rotation *vs.* $Cl_3/Cl_2(CO)$ planes) and the most stable (10–20°) ring orientation is consistent with this suggestion.

The Amsterdam Density Functional (ADF) package allows the total bonding energy to be broken down into steric and electronic components using the transition state procedure developed by Ziegler and others.[31–33] Fig. 8 presents the results of such an analysis for $[WCl_3(PH_3)_2(NPh)]$ **3′**. The total

bonding energy, steric repulsion and orbital interaction (electronic component) are all arbitrarily set to zero at the geometry in which the ring is in the plane of the three chlorine atoms (0° rotation), and their values at the other orientations are plotted relative to this point. It is immediately clear that the small differences in the total bonding energy from 0 to 90° arise from the virtual self-cancellation of the steric and electronic components. Up to a ring rotation of 50° neither of these components is greatly different from their value at 0°, but this changes significantly as the ring approaches coplanarity with the phosphine groups. The latter geometry is clearly favoured on electronic grounds but disfavoured sterically, and it is the steric repulsion that causes the 0° geometry to be favoured over the 90°.

(v) Electrochemical and spectroelectrochemical studies

In order to assess the degree of communication between metal centres in diimido-bridged complexes, the solution redox behaviour of ditungsten complexes **1a**, **1b**, **1g** and **1n**, **1o** and monomeric **1s** has been examined by cyclic voltammetry, differential pulse voltammetry and rotating disk voltammetry. At room temperature 0.5 mol dm^{-3} [^{n}Bu$_4$N][PF$_6$]–dichloromethane solutions of the ditungsten complexes each display an oxidation

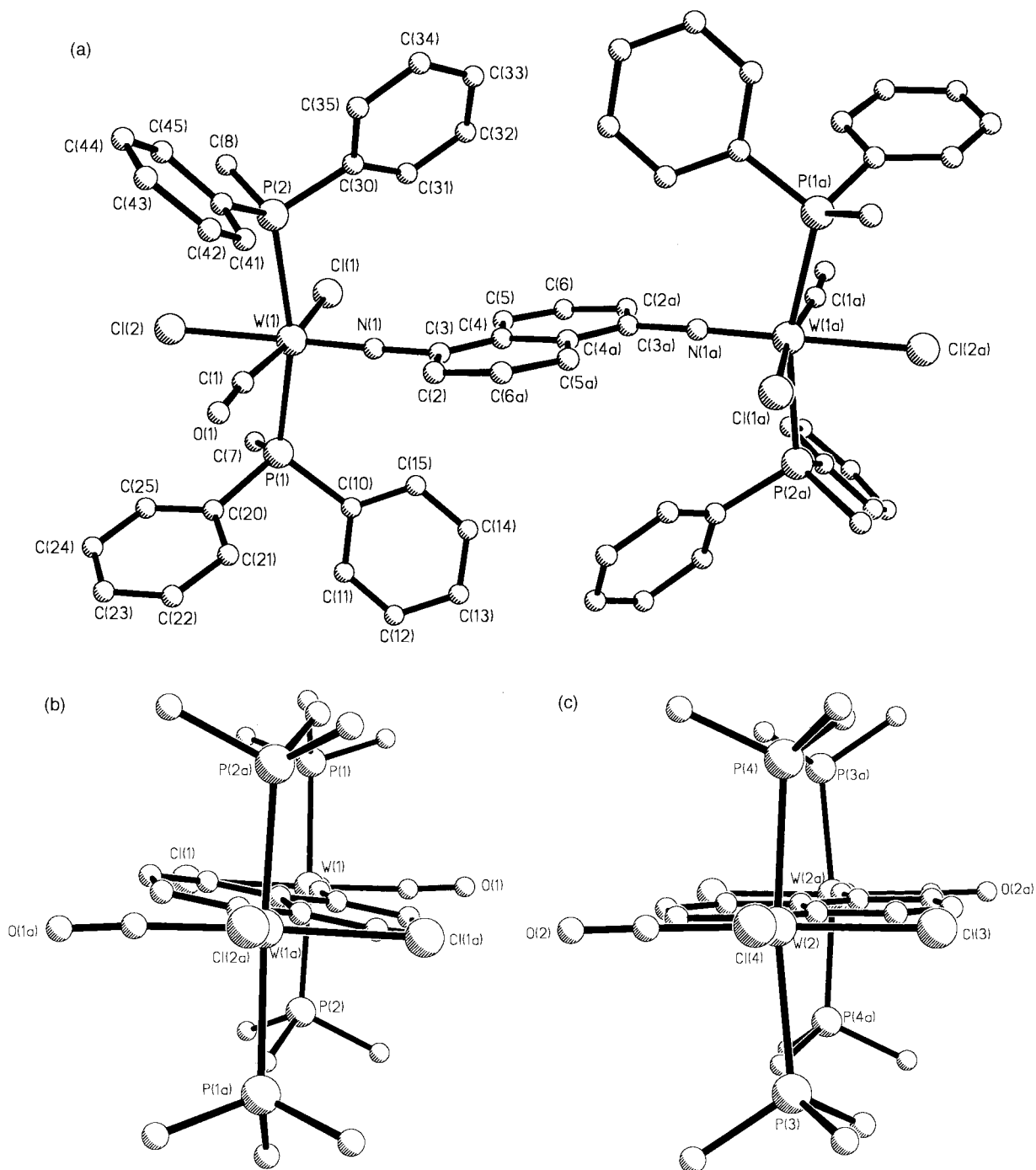**Fig. 4** Molecular structure of complex **1h** as in Fig. 3.

and a reduction, both of which are irreversible at scan rates up to 1000 mV s^{-1}. Similar behaviour is found with other solvents, *e.g.* 1,2-dichlorobenzene and propylene carbonate. Upon cooling the dichloromethane solutions to 213 K the oxidative processes for all ditungsten complexes and **1s** become chemically reversible thus permitting more detailed analysis of the voltammetric response. The reductive processes remain irreversible at low temperature for all but two of the complexes, namely **1a**, **1b**. For those, cooling of the solutions leads to the appearance of two waves which have some degree of chemical reversibility. Further discussion is limited to the results obtained at low temperature and these are summarised in Table 2.

Low temperature cyclic voltammograms of complex **1a** dissolved in 0.5 mol dm^{-3} [^{n}Bu$_4$N][PF$_6$]–dichloromethane are shown in Fig. 9. The scan to positive potentials reveals an oxidative response near +1.0 V, on which there is evidence for splitting of both the forward and return waves by the presence of a

shoulder on the leading edge of the forward wave, a feature mirrored in the return wave. By comparing the limiting current in a steady state voltammogram (obtained with a rotating disk electrode) with that for the oxidation of the monomeric complex **1s**, it has been established that the oxidation of **1a** (and all other bimetallic complexes) overall involves two electrons. The oxidative response is consistent with two closely spaced, one-electron oxidative processes, both of which have a high degree of chemical reversibility. Variable scan rate studies indicate that these processes are quasi-reversible in the electrochemical sense, in that the separation of the peaks in the forward and reverse scan increases with increasing scan rate. The small separation of the individual couples does not permit evaluation of peak-to-peak separation (ΔE_p) for each individual one-electron process. Similarly, the limiting currents for the oxidation and reduction, which is clearly resolved into two sequential one-electron processes (see later), are equal, such that the oxidation
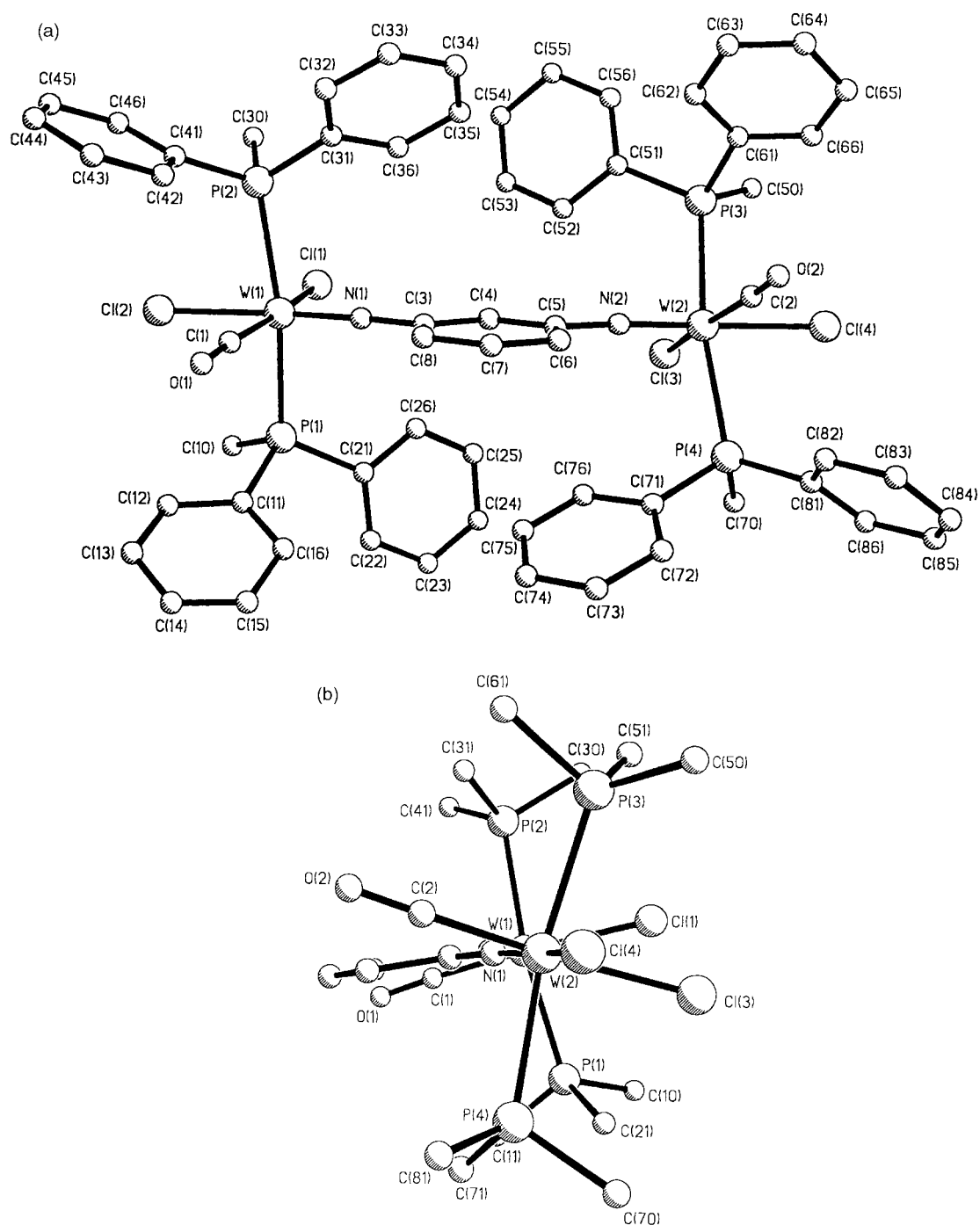
Fig. 5   Molecular structure of complex **1n** as in Fig. 1.

and reduction of the bimetallic complexes overall involves the same number of electrons. The results from differential pulse voltammetry are also consistent with the existence of two closely spaced oxidative waves, as shown by the asymmetry in the peak maximum. The individual oxidation potentials for the 36/35e and 35/34e couples have been estimated from differential pulse voltammograms, using the procedure of Taube and Richardson[34] and are listed in Table 2. The separation of the couples in **1n** is somewhat greater than that in isomeric **1a** as is evident from both the cyclic and differential pulse voltammograms, shown in Fig. 10. The oxidative response for the other bimetallic complexes are in general similar, with the exception of **1o**, which displays two couples that are clearly resolved.

Whilst the oxidative chemistry of the diimido-bridged ditungsten complexes is in general quite similar, the reductive chemistry is considerably different. At 213 K the phenylene-bridged complexes **1a**, **1b** display two well resolved reductions in the region -1.1 to -1.3 V, the first couple being more reversible than the second in the chemical sense. For the remainder of the complexes only a broad irreversible reduction in the region of -1.5 V is found. Steady-state voltammetry indicates that overall reduction of the bimetallic complexes involves two electrons.

In situ infrared spectroelectrochemical (IRSEC) studies have been conducted on complex **1a**, since its voltammetry offered the greatest promise of observing chemically reversible redox processes on the timescale of the IRSEC experiment. The oxidation of **1a** at $+1.2$ V in an infrared reflection absorption spectroscopic (IRRAS) cell at low temperature resulted in the collapse of the $v(CO)$ band due to the neutral complex at 1969 cm^{-1}, and the growth of a weak band at 2139 cm^{-1} which can be attributed to the formation of free CO. No other bands were observed that can be attributed to the formation of new tungsten carbonyl complexes. Returning the potential of the work-
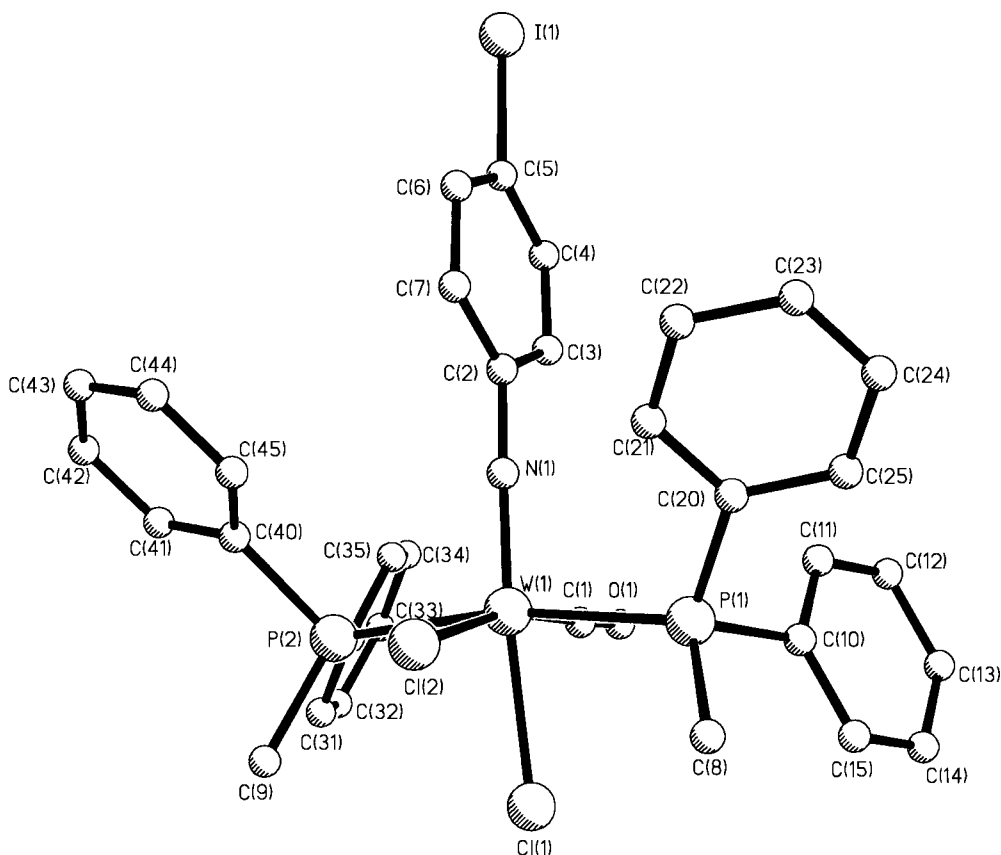
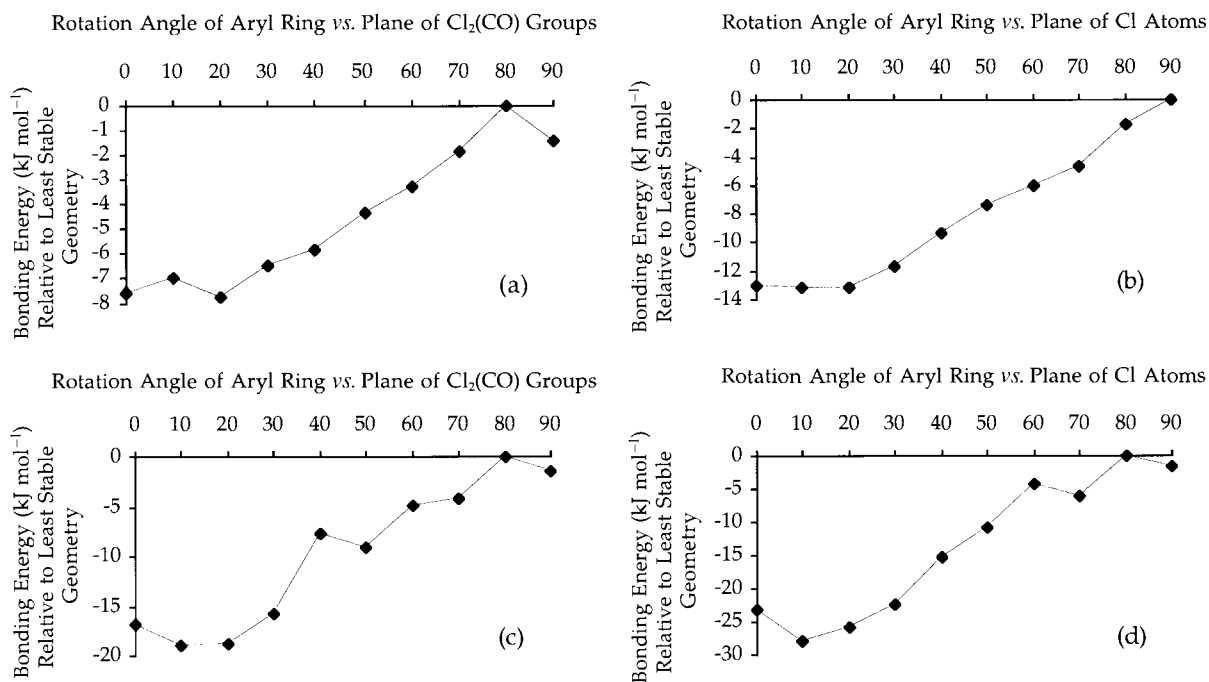**Fig. 6** Molecular structure of complex **1p**.

Fig. 7 Walsh diagrams for rotation of the aryl ring in (a) [WCl₂(PH₃)₂(CO)(NPh)] **1s′**, (b) [WCl₃(PH₃)₂(NPh)] **3′**, (c) [{WCl₂(PH₃)₂(CO)}₂-(μ-p-NC₆H₄)] **1a′**, (d) [{WCl₃(PH₃)₂}₂(μ-p-C₆H₄)] **2′**.

ing electrode to its initial rest value, *i.e.* 0.0 V, did not regenerate any of the neutral parent complex. Although the oxidation of **1a** appears chemically reversible on the timescale of the voltammetric experiment, on the timescale of an *in situ* infrared spectroelectrochemical experiment this process is chemically irreversible, with the decomposition of **[1a]⁺** (or **[1a]²⁺**) occurring through loss of CO. The species produced upon reduction of **1a** is equally unstable, in that the reduction is also chemically

irreversible. Reduction at −1.1 V led to the collapse of the *v*(CO) band and the growth of bands at 1729, 1685, 1627, 1581 and 1518 cm⁻¹. The higher wavenumber bands are more typical of bridging carbonyls, although the sharpness of some of the observed bands may indicate the formation of ketonic organic species. Given the instability of the redox products from **1a**, spectroelectrochemical studies of the other complexes were not undertaken.

**Table 1** Selected bond lengths (Å) and angles (°)

Complex		W–N	W–Cl[a]	W–Cl[b]	W–C	W–P	C–O	N–C	Cl–W–Cl	P–W–P	N–W–C	Torsion[c]	W–N–C
1a		1.743(5)	2.465(2)	2.466(2)	1.991(8)	2.528(2) 2.536(2)	1.145(11)	1.390(8)	90.0(1)	167.8(1)	87.91(3)	80.2	173.2(4)
1b		1.745(4)	2.4648(13)	2.4677(14)	1.986(6)	2.5243(14) 2.5339(14)	1.144(7)	1.388(6)	89.24(5)	166.19(4)	91.5(2)	10.2	176.6(4)
1g	Molecule A	1.7537(7)	2.477(3)	2.465(3)	1.991(12)	2.508(3) 2.536(3)	1.139(13)	1.374(12)	89.37(10)	166.34(10)	88.5(4)	26.1	171.3(7)
	Molecule B	1.758(8)	2.482(2)	2.466(3)	1.987(12)	2.508(4) 2.519(4)	1.153(13)	1.385(12)	89.45(9)	164.57(11)	88.8(4)	17.3	172.6(8)
1h	Molecule A	1.746(11)	2.446(4)	2.471(4)	1.99(2)	2.528(4) 2.550(4)	1.141(2)	1.44(2)	90.9(2)	163.65(12)	90.1(6)	10.7	172.4(10)
	Molecule B	1.757(13)	2.472(5)	2.445(4)	1.99(2)	2.536(4) 2.540(4)	1.13(2)	1.41(2)	86.7(2)	169.12(13)	92.5(7)	6.2	171.4(10)
1n		1.751(6)	2.462(2)	2.469(2)	1.993(9)	2.531(2) 2.537(2)	1.156(11)	1.1399(10)	90.7(1)	167.3(1)	88.2(3)	5.8	172.8(6)
		1.766(6)	2.460(3)	2.473(3)	1.997(9)	2.541(2) 2.537(2)	1.158(11)	1.381(10)	91.0(1)	167.5(1)	87.0(3)	23.9	172.4(5)
1p		1.752(7)	2.460(2)	2.454(2)	2.000(8)	2.521(2) 2.530(2)	1.138(9)	1.412(10)	88.86(8)	168.94(7)	88.9(3)	4.1	169.5(6)
1t[d]		1.754(6)			1.983(8)	2.521(2) 2.526(2)	1.139(8)		89.0(1)			4.3	171.6(5)
2[e]	Molecule A	1.735(8)	2.500(3)	2.395(3)		2.572(3) 2.550(3)		1.402(13)	85.7(1) 84.3(1)	171.5(8)		20.8	171.5(8)
	Molecule B	1.756(9)	2.508(3)	2.399(3)		2.573(3) 2.546(3)		1.357(14)	85.9(1) 84.0(1)	173.6(8)		31.8	173.6(8)

[a] *trans* to nitrogen. [b] *trans* to CO. [c] Plane of aryl ring(s) with respect to $Cl_2(CO)/Cl_3$ plane. [d] Ref. 22(a). [e] Ref. 11.

Table 2 Summary of electrochemical data

| Complex | $E^a_{1/2}/V$ | | | |
	$W^{IV}–W^V$	$W^V–W^V$	$W^{IV}–W^{III}$	$W^{III}–W^{III}$
1a	+1.07	+1.13	−1.08	−1.20
1b	+1.00	+1.09	−1.18	−1.30
1g[b]	+1.02	+1.08	≈−1.6	
1n[b]	+1.05	+1.16	≈−1.5	
1o[b]	+1.02	+1.19	≈−1.6	
1s[b,c]	+1.00		≈−1.7	

[a] Recorded in 0.5 mol dm^{-3} [^{n}Bu$_4$N][PF$_6$]–dichloromethane at 213 K $vs.$ Ag–AgCl against which ferrocenium–ferrocene is measured at +0.55 V. The $E_{1/2}$ potentials are estimated from differential pulse voltammograms, where $E_{1/2} = E_p \pm (MA/2)$ (MA = modulation amplitude), assuming that the couples are reversible. For the $W^{IV}–W^V$ and $W^V–W^V$ couples the individual $E_{1/2}$ potentials were estimated by the procedure of Taube and Richardson.[34] [b] Irreversible, E_{pc} quoted. [c] The monomeric complex **1s** displays one-electron processes; $E_{1/2} = (E_{pa} + E_{pc})/2$ taken from cyclic voltammetry.
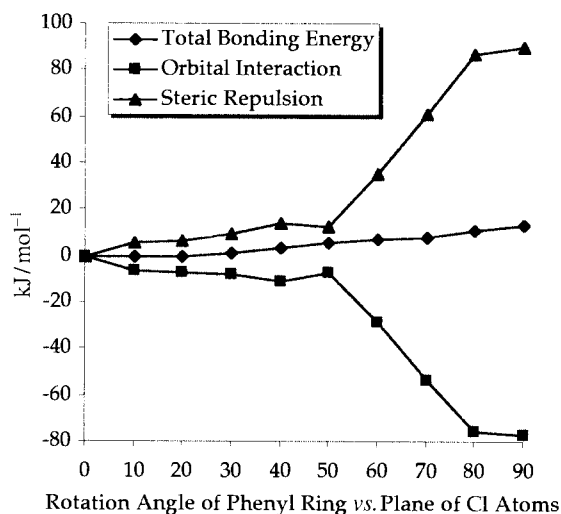
Fig. 8 Total binding energy, steric repulsion and orbital interaction upon phenyl ring rotation in complex **3′**.
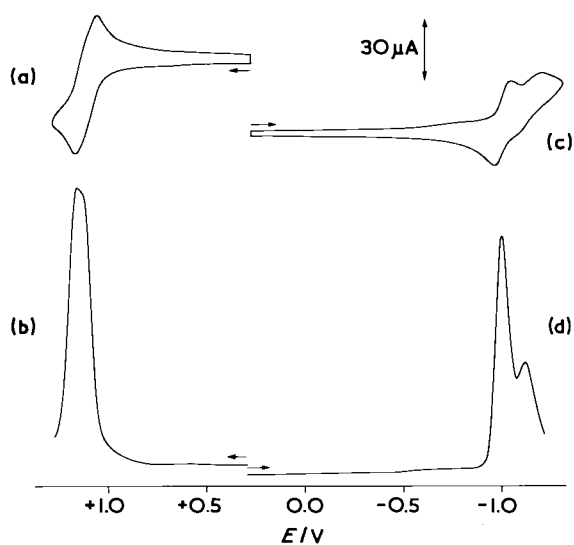
Fig. 9 Cyclic voltammetry (a,c) and differential pulse voltammetry (b,d) for complex **1a** at 213 K in dichloromethane.

(v) Electronic structure calculations: probing redox potentials

In order to probe further the electronic structure of diimidobridged complexes and to gain additional insight into the electrochemical and spectroelectrochemical studies, we have
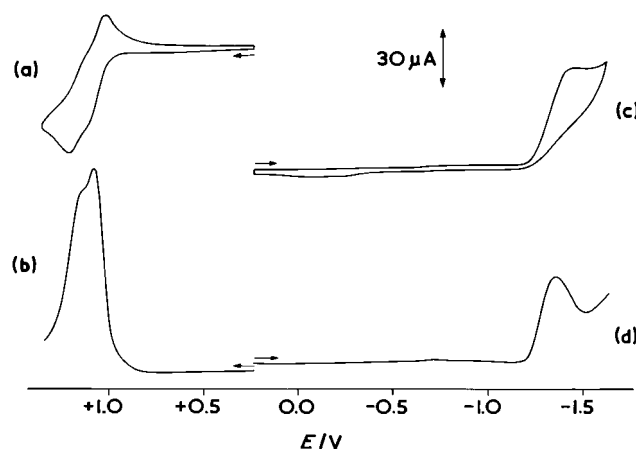

Fig. 10 Cyclic voltammetry (a,c) and differential pulse voltammetry (b,d) for complex **1n** at 213 K in dichloromethane.

conducted a series of density functional calculations on models for **1a**, **1b** and **1o** in which the Ph$_2$PMe ligands are replaced by PH$_3$ groups. In these calculations the atomic positions were taken from X-ray crystallographic data and idealised to the highest possible symmetry. Generally, this enforces symmetry equivalence of the metal atoms, thereby imposing delocalised bonding. This is anticipated to be a realistic approach to our studies, in that previous work, for example by McGrady *et al.*,[35] has shown that there is an increased tendency toward delocalisation with increasing atomic number in bimetallic systems such as [M$_2$Cl$_9$]$^{3-}$ (M = Cr, Mo or W) and [M$_2$Cl$_9$]$^-$ (M = Mn, Tc or Re).

Although there is not necessarily direct correlation between the calculated electronic structures of isolated molecules and solution electrochemistry data, it was our hope that analysis of the compositions and energies of the highest occupied and lowest unoccupied molecular orbitals (MOs) of the model compounds would aid our understanding of the experimental results. The electrochemical data reveal that all of the compounds studied display similar oxidation behaviour. Our calculations are consistent with this, in that the composition and energies of the highest occupied molecular orbital, from which the electrons are presumably removed in the oxidation process, are very similar in each of the model compounds. Fig. 11 presents plots of the highest occupied and lowest unoccupied MOs of **1a′** and **1o′**, from which it may be seen that the HOMOs are W–C bonding but C–O and W–Cl antibonding.† The W–C bonding character of the HOMO is consistent with the spectroelectrochemical observation that free CO is generated upon oxidation of **1a**. Removal of electron(s) from the HOMO will result in reduced W–C bonding, potentially leading to expulsion of CO from the complex.

Compounds **1a** and **1b** display reductive electrochemistry different from that of the other compounds studied. Again, this is consistent with our calculations, which reveal that the lowest unoccupied molecular orbital (LUMO) composition and energy relative to the HOMO is different in **1a′** and **1b′** in comparison with the other molecules. Thus, while the LUMO in **1a′** and **1b′** is 1.01 eV less stable than the HOMO, the HOMO–LUMO gap in **1o′** is 1.43 eV, consistent with the greater separation between the oxidation and reduction waves in **1o**. Fig. 11 clearly demonstrates that the composition of the LUMOs in **1a′** and **1o′** are different from one another, with no CO contribution to the LUMO of **1o′** and no C–C π interaction in the LUMO of **1a′**.

---

† Note that the higher symmetry (C_{2h}) of complex **1a′** forces equivalent contributions from both metal centres, while the HOMO and LUMO of the C_s symmetric **1o′** are concentrated on different ends of the molecule. The bonding characteristics of the HOMOs and LUMOs of both compounds are, however, very similar.
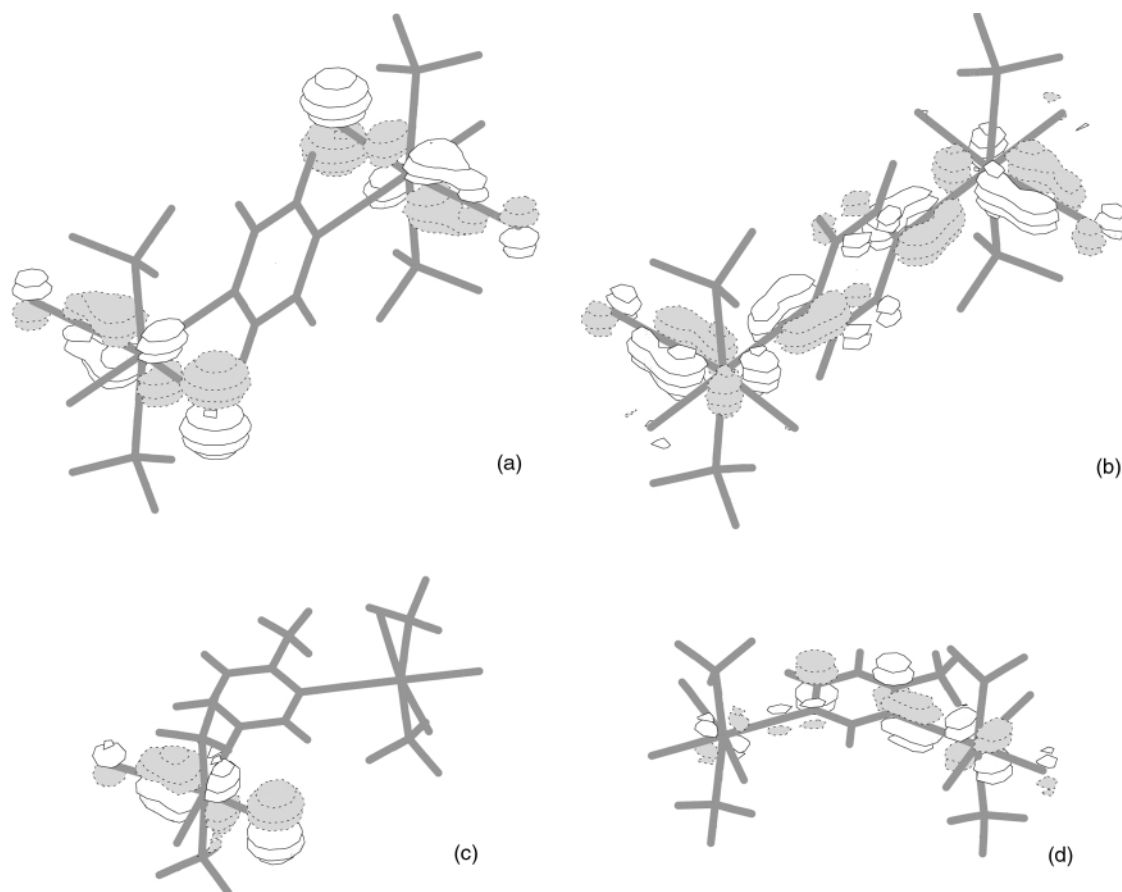
Fig. 11 MOLDEN plots of the highest occupied molecular orbital and lowest unoccupied molecular orbital for (a) complex **1a′** (HOMO), (b) **1a′** (LUMO), (c) **1o′** (HOMO), (d) **1o′** (LUMO).

The spectroelectrochemical behaviour of complex **1a** under reduction is more complicated than under oxidation, with the growth of several new bands and the collapse of ν(CO). Although our calculations do not fully explain this behaviour, it is noticeable that the LUMO of **1a′** is strongly W–N antibonding, and hence population of this orbital may be expected to result in the breaking of the W–N bonds. This is consistent with the observation that **1a** is unstable with respect to reduction in the spectroelectrochemical experiment.

Discussion

In a manner analogous to that developed by Mayer and co-workers,[22] oxidative addition of a range of π-conjugated diisocyanates **IIa–IIo** to two equivalents of [WCl$_2$(Ph$_2$PMe)$_4$] afforded a range of diimido-bridged tungsten(IV) complexes [{WCl$_2$(Ph$_2$PMe)$_2$(CO)}$_2$(μ-N–X–N)] **1a–1o** in good to moderate yield. Attempts to add a single tungsten centre to *para*-phenylene diisocyanate were unsuccessful resulting only in a 50:50 mixture of the double addition product **1a** and unchanged isocyanate. This suggests that co-ordination of one tungsten(IV) group to the isocyanate activates the second NCO group towards oxidative addition and provides some evidence of communication through the π-conjugated backbone. In related work concerning attempts to link molybdenum(VI) centres together *via* reaction of [MoOCl$_2$(S$_2$CNEt$_2$)$_2$] with *para*-phenylene diamines we found that co-ordination of the one molybdenum(VI) centre deactivated the second towards further metal co-ordination.[14] Both results provide evidence for communication through the π-conjugated framework, the deactivation of the amine resulting from delocalisation of the lone pair towards the electron-deficient molybdenum(VI) centre. The nature of the activation of the isocyanate by the tungsten(IV) centre is less clear. On the basis primarily of observations in

related ketone addition to **I** Bryan and Mayer[36] postulated that reactions proceed *via* a side-bound isocyanate, which subsequently undergoes oxidative addition. It is difficult to see how co-ordination of the tungsten(IV) centre can substantially effect the binding constant of the isocyanate. However, it may affect the rate of oxidative addition by virtue of weakening the nitrogen–carbon and strengthening the carbon–oxygen bond.

Reaction of 1,5-diisocyanatonaphthalene **IIh** with compound **I** proceeded somewhat differently to other diisocyanates. When followed by IR spectroscopy the isocyanate stretch at 2270 cm^{-1} decreased with the growth of two new absorptions; at 1964 cm^{-1} associated with the metal carbonyl moiety in **1h** and an unidentified band at 2094 cm^{-1}, which later disappeared. Attempts to isolate this intermediate were unsuccessful but it is tempting to speculate that it is the result of a side-bound isocyanate and indeed such species are known.[37] Again, the unusual behaviour of the 1,5-naphthalene linking unit seen here mirrors that found in the molybdenum(IV) diamine chemistry. Thus, deactivation of the second amine upon co-ordination of the first is not pronounced and allows the synthesis and characterisation of both monoimido [MoCl$_2$-(S$_2$CNEt$_2$)$_2$(1,5-NC$_{10}$H$_6$NH$_2$)] and diimido-bridged [{MoCl$_2$-(S$_2$CNEt$_2$)$_2$}$_2$(1,5-NC$_{10}$H$_6$N)] products.[14]

A second synthetic strategy towards diimido-bridged complexes *via* the attempted Ullman coupling of the mononuclear iodo-complex [WCl$_2$(Ph$_2$PMe)$_2$(CO)(*p*-NC$_6$H$_4$I)] **1p** was unsuccessful as was the attempted coupling of **1p** to *para*-amino-phenylethyne. The latter is somewhat surprising as Mayr and co-workers[28] recently showed that this is a useful strategy to derivatise tungsten alkylidyne complexes and possibly reflects the ease of reduction of the tungsten(IV) imido centre under the coupling conditions.

Characterisation of new tungsten(IV) imido complexes **1** was straightforward, six being analysed by X-ray crystallography.

Each tungsten centre consists of an approximately octahedral co-ordination sphere with *cis*-chlorides and *trans*-phosphines. The carbonyl and the imido ligands lie *cis* to one another, as expected for strong π-acceptor and donor ligands respectively, and as discussed fully in earlier papers by Mayer.[22] Structural differences between isomeric *para*- and *meta*-phenylene diimido-bridged complexes **1a** and **1n** have been discussed previously.[9] The major feature is a twisting out of the plane by 7.4° of the two tungsten centres in the *meta* isomer **1n**, while in *para*-**1a** they are related by a crystallographic inversion centre. The difference is probably due to increased steric crowding in **1n** as a result of the close proximity of the bulky tungsten centres.

For all complexes the major feature of interest is the orientation of the aryl ring(s) with respect to the other tungsten-bound ligands. Mayer has shown that in the monoimido complex [WCl$_2$(Ph$_2$PMe)$_2$(CO)(NC$_6$H$_4$Me-*p*)] **1t**[22a] the ring lies approximately in the WCl$_2$(CO) plane, an almost identical orientation to that in the *para*-iodo complex **1p**. Contrast this with the *para*-phenylene imido-bridged **1a** in which the aryl ring lies almost at right angles to the WCl$_2$(CO) plane, that is almost coplanar with the two phosphorus atoms and the tungsten centre. The initial surprise of this result is tempered by the observation that simple methyl substitution of the ring as in **1b** results in a reversion to the WCl$_2$(CO) plane. From these and other results (Table 1) it is clear that the aryl ring(s) can lie either in the WCl$_2$(CO) plane or at right angles to it, with intermediate orientations being disfavoured. For both biaryl-bridged **1g** and 1,5-naphthalene-bridged **1h** two crystallographically independent molecules result, the major differences between them being the aryl ring orientation. Thus in **1g** independent molecules are characterised by twists of 26.1 and 17.3° out of the WCl$_2$(CO) planes, with the former being the biggest deviation seen in all complexes. It thus appears from experimental data that there is a strong preference for the aryl ring(s) to lie in the WCl$_2$(CO) plane. As discussed previously by Mayer[22a] in this orientation the two filled W–N π orbitals are not of the same energy. That which lies in the W(CO) plane is stabilised *via* overlap of the p orbitals on nitrogen and the carbonyl carbon and thus it is the higher energy filled W–N π orbital parallel to this which overlaps better with the empty aromatic π* orbital(s) of the aryl ring. The difference in energy of the filled W–N π orbitals is expected to be small, being estimated at <9 kcal mol^{-1} from VT NMR measurements.[23] In order to probe this further we carried out a series of density functional calculations on model compounds with PH$_3$ ligands. From these it is clear that the most stable orientation of the aryl ring is that in which it lies in the WCl$_2$(CO) plane. It thus seems that the ring orientation found in **1a** is anomalous and may be the result of crystal packing forces. Complex **1a** cocrystallises with a molecule of chlorobenzene and although there are no intermolecular contacts between the two their preferred relative orientation may be enough to counter the relatively small energy difference between the most stable (in the Cl$_2$(CO)W plane) and least stable (at right angles to this) ring orientation. A closer look at the energy changes upon ring rotation reveals that between 0 and 30° neither steric nor electronic effects vary significantly, thus accounting for the differences seen within independent molecules of the same compound.

For the biaryl-bridged diimido complex **1g** a notable feature is the coplanarity of the aryl rings in both independent molecules. This is in accord with the situation in biphenyl in the solid-state.[38] In solution, however, biphenyl is known to prefer an orientation in which the dihedral angle between the two rings is 41.6°,[39] although the potential energy surface is very flat and the rotation barrier small. While we have no direct evidence of rotation about the linking carbon–carbon bond in **1g** we suppose that this is facile in solution. Studies on biphenyl have shown that the central carbon–carbon bond shortens upon both oxidation or reduction.[40] In **1g** this bond length of 1.49(2)

Å is almost identical to that found in neutral biphenyl [1.489 Å] suggesting that it is a simple single carbon–carbon bond.

A key aim of the work was to access the degree of communication between π-conjugated metal centres and this was undertaken by electrochemical studies and supported by electronic structure calculations. All complexes investigated showed similar oxidative behaviour, being reversible at low temperature by cyclic voltammetry. The oxidative response is consistent with two closely spaced, one-electron oxidations suggesting that there is some communication between the metal centres. Thus, peak-to-peak separations have been estimated from differential pulse voltammograms as 60 mV in **1a**, 90 mV in **1b**, 40 mV in **1g**, 110 mV in **1n** and 170 mV in **1o**, all of which are greater than the 36 mV separation expected on statistical grounds if both redox centres have identical $E_{1/2}$ values.[41] That the difference is greater in isomeric *meta* complexes **1n** and **1o** *versus para* complexes **1a** and **1b** is somewhat unexpected as communication between metal centres in the former is not allowed *via* a simple superexchange pathway. The slightly greater coupling in **1b** *versus* **1a** results from the inequivalence of the metal centres in the former, while as the chain length increases the interaction decreases as shown by the small value in **1g**. Spectroelectrochemical studies on **1a** reveal that oxidation results in CO loss and this is supported by calculations which show that the HOMO is W–C bonding in character.

While the oxidative chemistry is very similar for all compounds studied, the reductive chemistry is significantly different. *para*-Phenylene-bridged diimido complexes **1a** and **1b** both show two well resolved reductions, peak-to-peak separations being 120 mV for both, while in contrast other complexes showed only a broad irreversible reduction at high potential. This difference is supported by calculations, the HOMO–LUMO gap for **1a′** and **1b′** being significantly smaller than in the other complexes.

It is not easy to compare our results with those of others as only two preliminary reports of electrochemical studies on similar *para*-phenylene diimido bridged complexes have appeared.[10,13] In the Creutz–Taube ion the difference between the two oxidation potentials observed for the reduced isovalent system is 390 mV.[2] McCleverty, Jones and co-workers[42] have carried out detailed studies on 16-electron molybdenum nitrosyl systems bridged by a wide range of ligands; in 4,4′-bipyridyl bridged [{Mo(tp*)(NO)Cl}$_2$(4,4′-bipy)] [tp* = tris-(3,5-dimethylpyrazol-1-yl)hydroborate] reduction waves are separated by 765 mV.[42] Most closely related to our studies and specifically **1a** are their amido-bridged complexes [{M(tp*)-(NO)}$_2$(μ-*p*-NHC$_6$H$_4$NH)] in which redox processes are separated by 1.04 V (M = Mo) and 560 mV (M = W).[43] Clearly, this latter value is much greater than that of 120 mV found for **1a** and we conclude that at best the coupling between metal centres in imido-bridged complexes **1** is small. While the degree of communication between metal centres is clearly dependent upon the nature of the bridging ligand,[43,44] it is also a function of the distance between metal centres such that the metal–metal interaction decreases with increasing distance.[45] The difference in the oxidative responses of 60 mV for phenylene-bridged **1a** and 40 mV for biphenylene-bridged **1g** is in line with this, and as a result we did not try and assess the communication in complexes with longer bridges. Indeed, the value of 40 mV for **1g** is not significantly different to that expected if there were no communication.[41]

Experimental

General

Unless otherwise stated, all manipulations were carried out under nitrogen using standard vacuum line and glove-box techniques. Solvents were dried and degassed prior to use. Most diisocyanates and diamines were purchased from Aldrich,

Lancaster and Carbolabs and used without further purification. Phenylene diisocyanates and phenylenediamines were purified prior to use by vacuum sublimation using a tube furnace. Triphosgene, phosgene in toluene and [PdCl$_2$(PPh$_3$)$_2$] were purchased from Aldrich and used as supplied while [WCl$_2$(PPh$_2$Me)$_4$],[21] [WCl$_2$(Ph$_2$PMe)$_2$(CO)(NPh)] **1s**[22a] and *para*-ethynylaniline[23] were prepared *via* the literature methods. Chromatography was carried out on deactivated alumina (6% w/w distilled water) wet packed with light petroleum (bp 40–60 °C) unless otherwise stated. The solution to be separated was added to alumina (3–5 g) and the solvent removed under reduced pressure. The resulting solids were then deposited on top of the prepared column and separation effected by elution with progressively more polar solvents. Great caution was exercised when handling triphosgene, all manipulations being carried out in a well ventilated fume-hood and exit gases from the reaction and work-up were passed through a strong sodium hydroxide solution. The experimental procedure used is adapted from that described by Eckert and Forster[25] and solutions were routinely purged with nitrogen for at least 1 h after the reaction.

The IR spectra were recorded on a Nicolet 205 FTIR spectrometer, solid-state spectra being recorded as KBr discs, NMR spectra on Varian XL200 (^{1}H) or VXR400 (^{1}H, ^{13}C, ^{31}P) spectrometers and internally referenced to residual solvent peaks (^{1}H, ^{13}C) or externally to P(OMe)$_3$ (^{31}P) and mass spectra on VG 7070 high resolution and VG Analytical ZAB2F spectrometers. Elemental analyses were performed in house.

Electrochemistry

Voltammetric experiments utilised a single-compartment, three electrode cell, the electrodes consisting of a platinum bead working electrode, a platinum bar auxiliary electrode and a double-fritted Ag–AgCl reference electrode.[46] A PAR 174A Polarographic Analyser was used in conjunction with a PAR 175 Waveform Generator, without compensation for solution resistance. Rotating disk voltammetry employed a Metrohm Model 628-50 Pt rotating disk electrode. In 0.5 mol dm^{-3} [^{n}Bu$_4$N][PF$_6$]–dichloromethane solution the oxidation of ferrocene (Fc$^{0/+}$) at +0.55 V was used as an internal reference. Infrared spectroelectrochemical experiments utilised an IRRAS cell,[47] mounted in the sample compartment of a Nicolet Magna 750 FTIR spectrometer. Dichloromethane for electrochemical and spectroelectrochemical experiments was predried over KOH and distilled from CaH$_2$ just prior to use. The electrolyte was prepared by neutralisation of [^{n}Bu$_4$N]OH with HPF$_6$ and the crude product recrystallised twice from hot absolute ethanol before drying for 24 h *in vacuo* at 373 K.

Computational

All calculations were performed with the Amsterdam Density Functional program suite.[48,49] A triple-zeta, uncontracted Slater-type orbital valence basis set was employed for tungsten (ADF Type IV). Double-zeta bases were used for all the other atoms, together with a single polarisation function (ADF Type III). Quasi-relativistic scalar frozen cores were used for all the elements; C (1s), N (1s), O (1s), P (2p), Cl (2p) and W (5p). Relativistic core potentials were computed using the ADF auxiliary program "Dirac". The local density functional of Vosko, Wilk and Nusair[50] was used in all calculations. Both spin restricted and spin unrestricted (*i.e.* when α and β spin electrons of the same MO number and symmetry are not constrained to have the same spacial wavefunction) calculations were performed where appropriate. Bond lengths and angles were taken from the appropriate crystallographic data and the molecular geometry idealised to the highest possible symmetry. Molecular orbital plots were generated using the program MOLDEN, written by G. Schaftenaar of the COAS/CAMM Centre, Nijmegen. The ADF output files (TAPE21) were converted into MOLDEN format using the program ADFrom written by F. Mariotti of the University of Florence.[51]

Syntheses

Bis(4-aminophenyl)ethyne Il. Dried triethylamine (40 cm^3) was added to a mixture of *para*-iodoaniline (0.78 g, 3.56 mmol), copper(I) iodide (0.01 g, 0.06 mmol) and *para*-ethynylaniline (0.50 g, 4.27 mmol). The mixture was thoroughly degassed and heated to 50 °C in an oil-bath while stirring. After 10 min [PdCl$_2$(PPh$_3$)$_2$] (0.05 g, 0.07 mmol) was added and the mixture left at 50 °C for 20 min then brought to reflux for 20 min. Cooling to room temperature afforded a yellow solution with copious precipitate. Diethyl ether (75 cm^3) was added and the mixture was filtered in air to leave a white solid. This was redissolved in dichloromethane and prepared for chromatography on a column packed with hexane–benzene (3:2). Elution with dichloromethane gave a pale yellow band which afforded compound **Il** (0.21 g, 28%) as a pale yellow powder. Recrystallisation from hot benzene afforded yellow needles. IR (KBr): 3405, 3295 and 3195 cm^{-1} (NH). ^{1}H NMR (CDCl$_3$): δ 7.31 (d, J 8.0, 4 H, Ar), 6.63 (d, *J* 8.0 Hz, 4 H, Ar) and 3.78 (br, 4 H, NH$_2$). Mass spectrum (EI): *m/z* 208 (M$^+$). Calc. for C$_7$H$_6$N: C, 80.77; H, 5.77; N, 13.46. Found: C, 79.80; H, 5.75; N, 13.06%.

4-H$_2$NC$_6$H$_4$C≡CC$_6$H$_4$C≡CC$_6$H$_4$NH$_2$-4 Im. An analogous procedure was adopted to that described above using *para*-ethynylaniline (0.58 g, 4.96 mmol), 1,4-diiodobenzene (0.68 g, 2.06 mmol), copper(I) iodide (0.01 g, 0.06 mmol), [PdCl$_2$(PPh$_3$)$_2$] (0.058 g, 0.08 mmol) and triethylamine (40 cm^3) and yielded a cream solid. Chromatography gave a very slow moving yellow band with dichloromethane and thus acetone was added to hasten its removal. The yellow fraction eluted was evaporated to dryness to give orange compound **Im** (0.70 g, 55%). Recrystallisation from hot benzene afforded orange needles. IR (KBr): 3361 (NH), 2206 cm^{-1} (C≡C). ^{1}H NMR (CDCl$_3$): δ 7.45 (s, 4 H, Ar), 7.35 (d, *J* 8.0 Hz, 4 H, Ar), 6.65 (d, *J* 8.0 Hz, 4 H, Ar) and 3.80 (br, 4 H, NH$_2$). Mass spectrum (EI): *m/z* 308 (M$^+$). Calc. for C$_{22}$H$_{16}$N: C, 85.71; H, 5.19; N, 9.09. Found: C, 85.12; H, 5.65; N, 6.82%.

***para*-Aminodiphenylethyne Ir.** *para*-Iodoaniline (2.00 g, 9.13 mmol), copper(I) iodide (0.02 g, 0.09 mmol) and phenylethyne (1.17 g, 0.011 mmol) were placed in a Schlenk tube. Dried triethylamine (40 cm^3) was added and the contents were thoroughly degassed. To this yellow solution was added [PdCl$_2$(PPh$_3$)$_2$] (0.128 g, 0.183 mmol) and the resulting solution stirred overnight at room temperature. The solvent was removed under reduced pressure. Benzene (100 cm^3) extraction gave a yellow-brown solid which was chromatographed on a column made up from light petroleum–dichloromethane (1:1). Elution with dichloromethane gave an orange band which afforded compound **Ir** (1.27 g, 72%) as a yellow-orange powder. IR (KBr): 3476, 3381 (NH), 2211 cm^{-1} (C≡C). ^{1}H NMR (CDCl$_3$): δ 7.50 (d, *J* 8.0, 2 H, Ar), 7.34 (m, 5 H, Ar), 6.65 (d, *J* 8.0, 2 H, Ar) and 3.82 (br, 2 H, NH$_2$). Mass spectrum (EI): *m/z* 193 (M$^+$). Calc. for C$_{14}$H$_{11}$N: C, 87.05; H, 5.70; N, 7.25. Found: C, 86.75; H, 5.63; N, 7.16%.

2,3-Dimethylphenylene-1,4-diisocyanate IIc. 2,3-Dimethylphenylene-1,4-diamine **Ic** (0.25 g, 1.84 mmol) was dissolved in 1,2-dichlorobenzene (30 cm^3) to give a red solution which upon brisk addition of triphosgene (0.36 g, 1.22 mmol) became cloudy. A reflux condenser fitted with a bubbler was attached and on warming to reflux the solution became clear and purple. Reflux was maintained for 30 min and then cooling to room temperature yielded a yellow solution with some flocculent brown solid. After decanting the solution was purged vigorously with nitrogen for 45 min. Removal of the solvent under

reduced pressure at 40 °C gave an off-white solid. This was placed into a Schlenk flask fitted with a cold-finger and sublimation at 0.05 mmHg afforded compound **IIc** (0.15 g, 43%) as a white solid. IR (KBr): 2285 cm^{-1} (NCO). ^{1}H NMR (CDCl$_3$): δ 6.91 (s, 2 H, Ar) and 2.25 (s, 6 H, Me). Mass spectrum (EI): m/z 188 (M$^+$). Calc. for C$_5$H$_4$NO: C, 63.83; H, 4.26; N, 14.89. Found: C, 63.74; H, 4.27; N, 14.51%.

2,5-Dimethylphenylene-1,4-diisocyanate 2d. The procedure described above was followed using 2,5-dimethylphenylene-1,4-diamine **Id** (0.50 g, 3.97 mmol) in 1,2-dichlorobenzene (40 cm^3). The amine did not completely dissolve before triphosgene (0.73 g, 2.45 mmol) addition. Brilliant white compound **IId** (0.44 g, 59%) was sublimed from a green-brown sludge. IR (KBr): 2264 cm^{-1} (NCO). ^{1}H NMR (CDCl$_3$): δ 6.88 (s, 2 H, Ar) and 2.24 (s, 6 H, Me). Mass spectrum (EI): m/z 188 (M$^+$). Calc. for C$_5$H$_4$NO: C, 63.83; H, 4.26; N, 14.89. Found: C, 63.76; H, 4.19; N, 14.86%.

Tetramethylphenylene-1,4-diisocyanate IIe. A similar method was followed and from tetramethylphenylene-1,4-diamine **Ie** (0.50 g, 3.04 mmol) and triphosgene (0.60 g, 2.03 mmol) in 1,2-dichlorobenzene (30 cm^3), white compound **IIe** (0.50 g, 75%) was isolated. IR (KBr): 2285 cm^{-1} (NCO). ^{1}H NMR (CDCl$_3$): δ 2.26 (s, Me). Mass spectrum (EI): m/z 216 (M$^+$). Calc. for C$_6$H$_6$NO: C, 66.67; H, 5.56; N, 12.96. Found: C, 66.57; H, 5.54; N, 12.91%.

3,3′,5,5′-Tetramethylbiphenyl-4,4′-diisocyanate IIf. A similar method was followed and from 3,3′,5,5′-tetramethylbiphenyl-4,4′-diamine **If** (0.23 g, 0.96 mmol) and triphosgene (0.19 g, 0.64 mmol) in 1,2-dichlorobenzene (30 cm^3), white compound **IIf** (0.25 g, 90%) was isolated. IR (KBr): 2274 cm^{-1} (NCO). ^{1}H NMR (CDCl$_3$): δ 7.24 (s, 4 H, Ar) and 2.38 (s, 12 H, Me). Mass spectrum (EI): m/z 292 (M$^+$). Calc. for C$_9$H$_8$NO: C, 74.00; H, 5.48; N, 9.59. Found: C, 73.67; H, 5.36; N, 9.50%.

3,3′-Dimethoxybiphenyl-4,4′-diisocyanate IIg. Triphosgene (0.20 g, 0.68 mmol) was swiftly added to a red solution of 3,3′-dimethoxybiphenyl-4,4′-diamine **Ig** (0.25 g, 1.03 mmol) in 1,2-dichlorobenzene (30 cm^3). A reflux condenser with a bubbler fitted was attached. After a few minutes the solution became clear and lightened, then a blue hue formed. The mixture was brought to reflux over 40 min and maintained for 90 min. Cooling to room temperature afforded a colourless solution with some brown solid. The solution was decanted from the small amount of solid and purged vigorously with nitrogen for 1 h. The solvent was removed under reduced pressure to yield compound **IIg** (0.26 g, 85%) as a white solid. No further purification was attempted. IR (KBr): 2280 cm^{-1} (NCO). ^{1}H NMR (CDCl$_3$): δ 7.14 (m, 2 H, Ar), 7.04 (m, 4 H, Ar) and 3.99 (s, 6 H, OMe).

1,5-Diisocyanatonaphthalene IIh. A similar method was followed from naphthalene-1,5-diamine **Ih** (0.40 g, 2.53 mmol) and triphosgene (0.50 g, 1.69 mmol) in 1,2-dichlorobenzene (40 cm^3). Filtration was carried out while the reaction mixture was still warm and white compound **IIh** (0.12 g, 23%) was sublimed with some difficulty from an orange solid. IR (KBr): 2270 cm^{-1} (NCO). ^{1}H NMR (CDCl$_3$): δ 7.96 (d, J 8.6, 2 H, H^2 of Ar), 7.49 (t, J 8.0, 2 H, H^3 of Ar) and 7.36 (d, J 8.2 Hz, 2 H, H^4 of Ar). Mass spectrum (EI): m/z 210 (M$^+$). Calc. for C$_6$H$_3$NO, C, 68.57; H, 2.86; N, 13.33. Found: C, 67.02; H, 2.68; N, 12.87%.

Terphenyl-4,4″-diisocyanate IIi. A similar procedure was followed using terphenyl-4,4″-diamine **1i** (0.33 g, 1.27 mmol) in 1,2-dichlorobenzene (40 cm^3). Some dissolution was observed forming an ochre suspension. Triphosgene (0.25 g, 0.85 mmol) was added and the mixture heated at reflux for 3h. The solution was decanted after cooling and the solvent removed under reduced pressure to yield off-white compound **IIi** (0.08 g, 20%). No further attempt was made at purification. Attempts were made to extract more product from the remaining solid using hot toluene, however, these were unsuccessful. IR (KBr): 2265 cm^{-1} (NCO). ^{1}H NMR (CDCl$_3$): δ 7.63 (s, 4 H, Ar), 7.58 (d, J 8.0, 4 H, Ar), 7.26 (d, J 8.0, 4 H, Ar). Mass spectrum (EI): m/z 312 (M$^+$).

Bis(4-isocyanatophenyl)ethyne IIl. A mixture of bis(4-amino-phenyl)ethyne **Il** (0.29 g, 1.39 mmol), triethylamine (0.42 g, 4.16 mmol) and toluene (40 cm^3) was gently warmed to aid diamine dissolution. Triphosgene (0.28 g, 0.94 mmol) was added and standard reaction procedures were followed. Sublimation afforded compound **IIl** (0.16 g, 80%) as a pale yellow solid. IR (KBr): 2266 cm^{-1} (NCO). ^{1}H NMR (CDCl$_3$): δ 7.47 (d, J 8.0, 4 H, Ar) and 7.07 (d, J 8.0 Hz, 4 H, Ar). Mass spectrum (EI): m/z 260 (M$^+$).

4-OCNC$_6$H$_4$C≡CC$_6$H$_4$C≡CC$_6$H$_4$NCO-4 IIm. Diamine **Im** (0.20 g, 0.65 mmol), triethylamine (0.59 g, 5.84 mmol) and toluene (40 cm^3) were warmed gently to aid dissolution of the diamine. Triphosgene (0.13 g, 0.43 mmol) was added and the mixture refluxed for 2.5 h. After filtration, removal of solvent afforded compound **IIm** (0.04 g, 17%) as an orange solid. This did not sublime and no attempts were made at further purification. IR (KBr): 2284, 2253 cm^{-1} (NCO). ^{1}H NMR (CDCl$_3$): δ 7.51 (s, 4 H, Ar), 7.45 (d, J 8.0, 4 H, Ar) and 7.11 (d, J 8.0 Hz, 4 H, Ar). Mass spectrum (EI): m/z 360 (M$^+$).

***para*-Iodophenyl isocyanate IIp.** *para*-Iodoaniline (1.00 g, 4.57 mmol) was dissolved in toluene (30 cm^3) and triethylamine (1 cm^3) added. To this was added phosgene in toluene (24 cm^3, 46 mmol) *via* a syringe. Some cloudiness was seen and the mixture was heated to reflux for 30 min. The solvent was removed under reduced pressure and white compound **IIp** (0.62 g, 55%) isolated by sublimation. IR (KBr): 2283 and 2258 cm^{-1} (NCO). ^{1}H NMR (CDCl$_3$): δ 7.63 (d, J 8.4, 2 H, Ar) and 6.85 (d, J 8.4 Hz, 2 H, Ar). Mass spectrum (EI): m/z 245 (M$^+$).

***para*-OCNC$_6$H$_4$C≡CC$_6$H$_5$ IIr**. *para*-Aminodiphenylethyne **Ir** (0.33 g, 1.71 mmol), triethylamine (0.52 g, 5.13 mmol) and toluene (40 cm^3) were warmed in order to dissolve the amine and triphosgene (0.17 g, 0.57 mmol) was added. The solution was refluxed for 2 h. After cooling to room temperature and purging with nitrogen for 1 h, filtration gave an orange solution and a solid which was washed further with warm toluene (40 cm^3). The combined filtrates were evaporated to dryness to give an orange-brown solid from which sublimation afforded compound **IIr** (0.29 g, 77%) as a white powder. IR (KBr): 2263 (NCO), 2124 cm^{-1} (C≡C). ^{1}H NMR (d^6-acetone): δ 7.6–7.2 (m, Ar). Mass spectrum (EI): m/z 219 (M$^+$).

[{WCl$_2$(Ph$_2$PMe)$_2$(CO)}$_2$(μ-*p*-NC$_6$H$_4$N)] Ia. In a glove-box, [WCl$_2$(Ph$_2$PMe)$_4$] (2.00 g, 1.90 mmol) and *p*-phenylene-1,4-diisocyanate (0.15 g, 0.95 mmol) were placed in a Schlenk tube. After removal from the box, toluene (30 cm^3) was added *via* a cannula and the mixture stirred at room temperature for 3 h. The initially orange solution progressively darkened over this period becoming green-brown and all solids dissolved. The volume was reduced under reduced pressure to approximately 5 cm^3 and light petroleum (30 cm^3) added. A green solid precipitated which was filtered off and washed with light petroleum (10 cm^3). Elemental analysis was obtained on this solid. Dissolution in dichloromethane (5 cm^3) in air gave a dark green solution. This was layered with methanol (10 cm^3), slow diffusion of the two solids depositing complex **1a** (1.50 g, 93%) as a green powder. Attempts to grow good quality single crystals from a variety of organic solvents led only to the formation of fine and brittle needles. However, slow evaporation of a 1,4-dichlorobenzene solution afforded large green blocks suitable for X-ray crystallography. IR (KBr): 1960vs (CO), 1486m,

1438m, 1432m, 1346w, 1100w, 890s, 846w, 742s, 693s, 504m and 455w cm^{-1}. ^{1}H NMR (CDCl$_3$): δ 7.67–7.17 (m, 40 H, Ph), 5.95 (s, 4 H, Ar) and 2.28 (t, J 3.9 Hz, 12 H, Me). ^{13}C NMR (CDCl$_3$): δ 239.8 (s, CO), 151.7 (s), 135.4 (t, 22.8), 134.0 (t, J 20.5), 133.0 (t, J 5.5), 131.9 (t, J 5.2), 130.0 (s), 129.9 (s), 128.9 (s), 128.2 (t, J 4.8), 128.1 (t, J 4.8 Hz) and 124.7 (s). ^{31}P NMR (CDCl$_3$): δ 2.08 (s, J_{PW} 290 Hz). Mass spectrum (FAB): m/z 1442 (M$^+$ − CO) and 1414 (M$^+$ − 2CO). Calc. for C$_{60}$H$_{56}$Cl$_4$N$_2$O$_2$-P$_4$W$_2$·C$_7$H$_8$: C, 51.47; H, 4.10; N, 1.79; P, 7.93. Found: C, 51.56; H, 4.07; N, 1.80; P, 7.97%.

For other complexes **1** a similar procedure was adopted unless otherwise stated.

[{WCl$_2$(Ph$_2$PMe)$_2$(CO)}$_2$(μ-p-N-o-MeC$_6$H$_3$N)] 1b. Reaction of [WCl$_2$(Ph$_2$PMe)$_4$] (1.10 g, 1.16 mmol) and 2-methyl-phenylene-1,4-diisocyanate **IIb** (0.1 g, 0.58 mmol) in toluene (35 cm^3) gave complex **1b** (0.73 g, 85%). Crystals suitable for X-ray analysis were grown from dichloromethane–methanol mixtures in air. IR (KBr): 1968vs (CO), 1483w, 1435s, 1098w, 891s, 738m, 693s and 507m cm^{-1}; ^{1}H NMR (CDCl$_3$): δ 7.78–6.94 (m, 40 H, Ph), 6.14 (d, J 8.2, 1 H, Ar), 5.94 (d, J 8.2, 1 H, Ar), 5.74 (s, 1 H, Ar), 2.33 (t, J 4.2, 3 H, Me) and 2.29 (t, J 4.3 Hz, 12 H, Me). ^{13}C NMR (CDCl$_3$): δ 243.2 (s, CO), 239.4 (s, CO), 151.6 (s), 150.5 (s), 135.5 (t, J 27.2), 134.2 (t, J 22.7), 133.4 (t, J 5.1), 132.4 (t, J 5.1), 132.1 (t, J 4.7), 131.9 (t, J 4.7), 130.1 (s), 130.0 (s), 129.5 (s), 128.3 (s), 127.8 (t, J 4.2), 126.0 (m), 122.5 (s), 17.0 (s, Me), 13.5 (t, J 15.3, Me) and 13.3 (t, J 15.7 Hz). ^{31}P NMR (CDCl$_3$): δ 3.43 (s, J_{PW} 291) and 2.06 (s, J_{PW} 291 Hz). Mass spectrum (FAB): m/z 1455 (M$^+$ − CO). Calc. for C$_{61}$H$_{58}$Cl$_4$P$_4$N$_2$O$_2$W$_2$·CH$_3$OH: C, 49.08; H, 3.83; N, 1.85. Found: C, 49.10; H, 3.90; N, 1.86%.

[{WCl$_2$(Ph$_2$PMe)$_2$(CO)}$_2$(μ-p-N-2,3-Me$_2$C$_6$H$_2$N)] 1c. Reaction of [WCl$_2$(Ph$_2$PMe)$_4$] (0.12 g, 0.11 mmol) and 2,3-dimethyl-phenylene-1,4-diisocyanate **IIc** (0.011 g, 0.06 mmol) in toluene (10 cm^3) gave complex **1c** (0.035 g, 40%). IR (KBr): 1965vs cm^{-1} (CO). ^{1}H NMR (CDCl$_3$): δ 7.67–6.80 (m, 42 H, Ph + Ar), 2.30 (t, J 4.0 Hz, 12 H, Me) and 1.24 (s, 6 H, Me). ^{31}P NMR (CDCl$_3$): δ 2.30 (s, J_{PW} 292 Hz). Mass spectrum (FAB): m/z 1499 (M$^+$). Calc. for C$_{31}$H$_{30}$Cl$_2$NOP$_2$W: C, 49.73; H, 4.01; N, 1.87. Found: C, 49.42; H, 3.89; N, 1.86%.

[{WCl$_2$(Ph$_2$PMe)$_2$(CO)}$_2$(μ-p-N-2,5-Me$_2$C$_6$H$_2$N)] 1d. Reaction of [WCl$_2$(Ph$_2$PMe)$_4$] (0.45 g, 0.43 mmol) and 2,5-dimethyl-phenylene-1,4-diisocyanate **IId** (0.04 g, 0.21 mmol) in toluene (10 cm^3) gave complex **1d** (0.23 g, 74%). IR (KBr): 1954vs cm^{-1} (CO). ^{1}H NMR (CDCl$_3$): δ 7.57–7.00 (m, 40 H, Ph), 6.02 (s, 2 H, Ar), 2.28 (t, J 4.0 Hz, 12 H, Me) and 1.27 (s, 6 H, Me). ^{13}C NMR (CDCl$_3$): δ 243.0 (s, CO), 150.4 (s), 135.4 (t, J 22.8), 134.2 (t, J 23.9), 132.7 (s), 132.4 (t, J 5.3), 132.2 (t, J 5.3), 130.1 (s), 129.7 (s), 128.2 (t, J 4.8), 127.9 (t, J 4.7), 127.8 (s), 16.5 (s, Me) and 13.3 (t, J 15.5 Hz, Me). ^{31}P NMR (CDCl$_3$): δ 2.20 (s, J_{PW} 292 Hz). Mass spectrum (FAB): m/z 1470 (M$^+$ − CO). Calc. for C$_{31}$H$_{30}$Cl$_2$NOP$_2$W: C, 49.73; H, 4.01; N, 1.87. Found: C, 49.42; H, 3.84; N, 1.89%.

[{WCl$_2$(Ph$_2$PMe)$_2$(CO)}$_2$(μ-p-NMe$_4$C$_6$N)] 1e. Reaction of [WCl$_2$(Ph$_2$PMe)$_4$] (0.43 g, 0.40 mmol) and tetramethyl-phenylene-1,4-diisocyanate **IIe** (0.034 g, 0.20 mmol) in toluene (40 cm^3) after overnight stirring gave complex **1e** (0.20 g, 66%). IR (KBr): 1956vs cm^{-1} (CO). ^{1}H NMR (CDCl$_3$): δ 7.95–6.85 (m, 40 H, Ph), 2.29 (t, J 4.0 Hz, 12 H, Me) and 1.54 (s, 12 H, Me). ^{31}P NMR (CDCl$_3$): δ 2.80 (s, J_{PW} 292 Hz). Mass spectrum (FAB): m/z 1498 (M$^+$ − CO). Calc. for C$_{32}$H$_{32}$Cl$_2$NOP$_2$W: C, 50.33; H, 4.32; N, 1.83. Found: C, 51.52; H, 4.51; N, 1.68%.

[{WCl$_2$(Ph$_2$PMe)$_2$(CO)}$_2$(μ-p-N-3,3′,5,5′-Me$_4$C$_{12}$H$_4$N)] 1f. Reaction of [WCl$_2$(Ph$_2$PMe)$_4$] (0.43 g, 0.40 mmol) and 3,3′,5,5′-tetramethylbiphenyl-4,4′-diisocyanate **IIf** (0.06 g, 0.21 mmol) in toluene (40 cm^3) gave complex **1f** (0.19 g, 56%). IR (KBr):

1953vs cm^{-1} (CO). ^{1}H NMR (CDCl$_3$): δ 8.00–7.08 (m, 40 H, Ph), 6.74 (s, 4 H, Ar), 2.31 (t, J 4.0, 12 H, Me) and 1.64 (s, 12 H, Me). ^{13}C NMR (CDCl$_3$): δ 241.2 (s, CO), 155.5 (s), 135.8 (t, J 22.8), 134.6 (t, J 21.7), 133.1 (t, J 5.3), 132.3 (t, J 5.3), 129.8 (t, J 4.5), 125.9 (t, J 4.7), 126.2 (s), 19.2 (s, Me), 17.9 (s, Me) and 13.5 (t, J 15.5, Me). ^{31}P NMR (CDCl$_3$): δ 2.20 (s, J_{PW} 293 Hz). Mass spectrum (FAB): m/z 1574 (M$^+$ − CO). Calc. for C$_{35}$H$_{34}$-Cl$_2$NOP$_2$W·CH$_2$Cl$_2$: C, 48.76; H, 4.06; N, 1.58. Found: C, 48.66; H, 3.91; N, 1.52%.

[{WCl$_2$(Ph$_2$PMe)$_2$(CO)}$_2$(μ-p-N-3,3′-(MeO)$_2$C$_{12}$H$_6$N)] 1g. Reaction of [WCl$_2$(Ph$_2$PMe)$_4$] (0.71 g, 0.68 mmol) and 3,3′-dimethoxybiphenyl-4,4′-diisocyanate **IIg** (0.10 g, 0.33 mmol) in toluene (40 cm^3) gave complex **1g** (0.48 g, 88%). Crystals suitable for X-ray analysis were grown upon slow diffusion of methanol into a saturated dichloromethane solution. IR (KBr): 1975vs (CO), 1591m, 1545w, 1483m, 1435s, 1392w, 1283w, 1241w, 1100m, 1021m, 889s, 805m, 742m, 692s and 506m cm^{-1}. ^{1}H NMR (CDCl$_3$): δ 7.69–7.24 (m, 40 H, Ph), 6.57 (d, J 8.4, 2 H, Ar), 6.54 (s, 2 H, Ar), 6.53 (d, J 8.4, 2 H, Ar), 3.56 (s, 6 H, MeO) and 2.31 (t, J 4.0 Hz, 12 H, Me). ^{13}C NMR (CDCl$_3$): δ 238.1 (s), 155.5 (s), 143.5 (s), 139.5 (s), 135.7 (t, J 20.8), 134.5 (t, J 21.1), 133.1 (t, J 5.3), 132.3 (t, J 5.2), 129.7 (d, J 11.5), 128.0 (m), 125.9 (s), 117.9 (s), 108.7 (s), 54.5 (s, MeO) and 13.5 (t, J 15.2 Hz, Me). ^{31}P NMR (CDCl$_3$): δ 3.20 (s, J_{PW} 292 Hz). Mass spectrum (FAB): m/z 1578 (M$^+$ − CO). Calc. for C$_{34}$H$_{32}$Cl$_2$NO$_2$P$_2$W: C, 50.81; H, 3.99; N, 1.74. Found: C, 50.87; H, 4.18; N, 1.85%.

[{WCl$_2$(Ph$_2$PMe)$_2$(CO)}$_2$(μ-1,5-NC$_{10}$H$_6$N)] 1h. Reaction of [WCl$_2$(Ph$_2$PMe)$_4$] (0.25 g, 0.24 mmol) and 1,5-diisocyanato-naphthalene **Ih** (0.025 g, 0.12 mmol) in toluene (20 cm^3) gave complex **1h** (0.10 g, 55%) as a green powder after several recrystallisations from methanol–dichloromethane mixtures. IR (KBr): 1964vs cm^{-1} (CO). ^{1}H NMR (CDCl$_3$): δ 7.83–6.94 (m, 46 H, Ph + Ar) and 2.31 (t, J 4.0 Hz, 12 H, Me). ^{31}P NMR (CDCl$_3$): δ 3.00 (s, J_{PW} 292 Hz). Mass spectrum (FAB): m/z 1492 (M$^+$ − CO). Calc. for C$_{64}$H$_{58}$Cl$_4$N$_2$O$_4$P$_4$W$_2$·0.5CH$_2$Cl$_2$: C, 49.54; H, 3.78; N, 1.79. Found: C, 49.22; H, 3.83; N, 1.76%.

[{WCl$_2$(Ph$_2$PMe)$_2$(CO)}$_2$(μ-p-N(C$_6$H$_4$)$_3$N)] 1i. Reaction of [WCl$_2$(Ph$_2$PMe)$_4$] (0.41 g, 0.39 mmol) and terphenylene-4,4″-diisocyanate **IIi** (0.06 g, 0.19 mmol) in toluene (30 cm^3) gave complex **1i** (0.10 g, 55%). IR (KBr): 1954vs cm^{-1} (CO). ^{1}H NMR (CDCl$_3$): δ 7.78–7.31 (m, 44 H, Ph + Ar), 7.17 (d, J 8.5, 4 H, Ar), 6.51 (d, J 8.5, 4 H, Ar) and 2.34 (t, J 4.0, 12 H, Me). ^{13}C NMR (CDCl$_3$): δ 240.1 (s, CO), 153.9 (s), 139.2 (s), 137.8 (s), 135.5 (t, J 22.9), 134.2 (t, J 21.0), 133.2 (t, J 5.0), 132.1 (t, J 5.0), 130.0 (s), 129.7 (s), 128.3 (d, J 4.8), 127.2 (s), 126.6 (s), 126.5 (s), 125.6 (s) and 13.6 (t, J 14.1 Hz, Me). ^{31}P NMR (CDCl$_3$): δ 3.10 (s, J_{PW} 292 Hz). Mass spectrum (FAB): m/z 1594 (M$^+$ − CO). Calc. for C$_{72}$H$_{64}$Cl$_4$N$_2$O$_4$P$_4$W$_2$·CH$_2$Cl$_2$: C, 51.30; H, 3.87; N, 1.64. Found: C, 50.77; H, 3.73; N, 1.70%.

[{WCl$_2$(Ph$_2$PMe)$_2$(CO)}$_2$(μ-p-NC$_6$H$_4$CH$_2$C$_6$H$_4$N)] 1j. Reaction of [WCl$_2$(Ph$_2$PMe)$_4$] (0.25 g, 0.24 mmol) and methylene-diphenylene-4,4′-diisocyanate **IIj** (0.03 g, 0.12 mmol) in toluene (20 cm^3) gave purple complex **1j** (0.16 g, 85%). IR (KBr): 1962vs cm^{-1} (CO). ^{1}H NMR (CDCl$_3$): δ 7.72–7.22 (m, 40 H, Ph), 6.58 (d, J 8.2, 4 H, Ar), 6.35 (d, J 8.2, 4 H, Ar), 3.57 (s, 2 H, CH$_2$) and 2.31 (t, J 4.0, 12 H, Me). ^{13}C NMR (CDCl$_3$): δ 240.2 (s, CO), 153.6 (s), 139.3 (s), 136.2 (t, J 20.9), 134.9 (t, J 20.5), 133.9 (t, J 5.1), 132.8 (t, J 5.2), 130.7 (t, J 3.4), 129.3 (s), 129.0 (d, J 4.5), 128.9 (d, J 5.0), 125.9 (s), 41.4 (s, CH$_2$) and 13.5 (t, J 15.2 Hz, Me). ^{31}P NMR (CDCl$_3$): δ 3.20 (s, J_{PW} 292 Hz). Mass spectrum (FAB): m/z 1532 (M$^+$ − CO). Calc. for C$_{67}$H$_{62}$Cl$_4$N$_2$O$_4$-P$_4$W$_2$: C, 51.54; H, 3.97; N, 1.80. Found: C, 51.60; H, 4.16; N, 1.86%.

[{WCl$_2$(Ph$_2$PMe)$_2$(CO)}$_2$(μ-p-NC$_6$H$_{10}$CH$_2$C$_6$H$_{10}$N)] 1k. Reaction of [WCl$_2$(Ph$_2$PMe)$_4$] (0.32 g, 0.31 mmol) and bis(4-iso-

cyanatocyclohexyl)methane **IIk** (0.04 g, 0.15 mmol) in toluene (20 cm³) gave purple complex **1k** (0.21 g, 90%). IR (KBr): 1961vs cm⁻¹ (CO). ¹H NMR (CDCl₃): δ 7.88–7.38 (m, 40 H, Ph), 3.46 (q, J 8.0, 2 H, CH₂), 2.31 (t, J 4.0 Hz, 12 H, Me) and 1.20–0.52 (m, 20 H, Cy). ³¹P NMR (CDCl₃): δ 3.20 (s, J$_{PW}$ 292). Mass spectrum (FAB): m/z 1543 (M⁺ − CO). Calc. for C₇₇H₆₂Cl₄N₂O₄P₄W₂: C, 51.15; H, 4.71; N, 1.78. Found: C, 50.59; H, 4.63; N, 1.76%.

[{WCl₂(Ph₂PMe)₂(CO)}₂(μ-p-NC₆H₄C≡CC₆H₄N)] 1l. Reaction of [WCl₂(Ph₂PMe)₄] (0.40 g, 0.38 mmol) and bis(4-isocyanatophenyl)ethyne **III** (0.05 g, 0.19 mmol) in toluene (20 cm³) for 2d at room temperature gave a purple solution and an off-white solid. After filtration and removal of most of the solvent under reduced pressure light petroleum (10 cm³) was added to give a green precipitate. This was redissolved in dichloromethane (ca. 1 cm³) and addition of methanol gave green complex **1l** (0.17 g, 57%). IR (KBr): 1965vs cm⁻¹ (CO). ¹H NMR (CDCl₃): δ 7.67–6.80 (m, 48 H, Ph + Ar) and 2.31 (t, J 4.0 Hz, 12 H, Me). ³¹P NMR (CDCl₃): δ 3.00 (s, J$_{PW}$ 292 Hz). Mass spectrum (FAB): m/z 1540 (M⁺ − CO).

[{WCl₂(Ph₂PMe)₂(CO)}₂(μ-p-NC₆H₄C≡CC₆H₄C≡CC₆H₄N)] 1m. Reaction of [WCl₂(Ph₂PMe)₄] (0.40 g, 0.38 mmol) and diamine **IIm** (0.04 g, 0.15 mmol) in toluene (40 cm³) for 3d resulted in the slow dissolution of most solids. After filtration the solvent was reduced to ca. 2 cm³ and light petroleum (10 cm³) added to effect precipitation of green complex **1m** (0.14 g, 44%). IR (CH₂Cl₂): 1966vs cm⁻¹ (CO). ¹H NMR (CDCl₃): δ 7.73–6.87 (m, 52 H, Ph + Ar) and 2.31 (t, J 4.0 Hz, 12 H, Me). ³¹P NMR (CDCl₃): δ 3.00 (s, J$_{PW}$ 292). Mass spectrum (FAB): m/z 1642 (M⁺ − CO).

[{WCl₂(Ph₂PMe)₂(CO)}₂(μ-m-NC₆H₄N)] 1n. Reaction of [WCl₂(Ph₂PMe)₄] (0.53 g, 0.50 mmol) and meta-phenylenediisocyanate **IIn** (0.04 g, 0.25 mmol) in toluene (35 cm³) for 1d gave a purple solution. Removal of solvent under reduced pressure afforded an oily solid which was washed with light petroleum. Redissolution in dichloromethane and addition of methanol afforded purple complex **1n** (0.33 g, 89%). Cooling a saturated THF solution to −40 °C gave crystals suitable for X-ray analysis. IR (CH₂Cl₂): 1966vs cm⁻¹ (CO). ¹H NMR (CDCl₃): δ 7.60–6.95 (m, 40 H, Ph), 6.35 (t, J 8.1, 1 H, Ar), 6.10 (d, J 8.1, 2 H, Ar), 6.00 (s, 1 H, Ar) and 2.24 (t, J 3.9 Hz, 12 H, Me). ¹³C NMR (CDCl₃): δ 239.5 (s, CO), 153.9 (s), 135.3 (t, J 22.9), 133.8 (t, J 20.7), 132.9 (t, J 5.1), 132.0 (t, J 5.1), 130.1 (s), 128.3 (t, J 4.5), 128.1 (t, J 4.7), 123.5 (s), 119.5 (s) and 13.5 (t, J 15.5 Hz, Me). ³¹P NMR (CDCl₃): δ 2.14 (s, J$_{PW}$ 290 Hz). Mass spectrum (FAB): m/z 1442 (M⁺ − CO). Calc. for C₆₀H₅₆Cl₄N₂O₂P₄W₂·0.5CH₂Cl₂: C, 48.00; H, 3.77; P, 8.20; Cl, 11.73; N, 1.85. Found: C, 47.81; H, 3.85; Cl, 11.16; N, 1.84, P, 8.55%.

[{WCl₂(Ph₂PMe)₂(CO)}₂(μ-m-N-4-MeC₆H₃N)] 1o. Reaction of [WCl₂(Ph₂PMe)₄] (0.20 g, 0.19 mmol) and 4-methyl-meta-phenylenediisocyanate **IIo** (0.017 g, 0.09 mmol) in toluene (35 cm³) for 1 d gave a claret solution. Removal of solvent under reduced pressure afforded an oily solid which was washed with light petroleum. Redissolution in dichloromethane and addition of methanol gave purple complex **1o** (0.13 g, 92%). IR (KBr): 1966s (CO), 1961s (CO), 1481m, 1432m, 1340w, 1315w, 1271w, 1095m, 895s, 891s, 734m, 730m, 693s, 498m, 488w and 450m cm⁻¹. ¹H NMR (CDCl₃): δ 7.78–6.75 (m, 40 H, Ph), 6.14 (s, 2 H, Ar), 6.09 (s, 1 H, Ar), 2.26 (t, J 3.9, 6 H, Me), 2.24 (t, J 4.0 Hz, 6 H) and 1.55 (s, 3 H, Me). ³¹P NMR (CDCl₃): δ 3.30 (s, J$_{PW}$ 291) and 2.20 (s, J$_{PW}$ 291 Hz). Mass spectrum (FAB): m/z 1456 (M⁺ − CO). Calc. for C₆₁H₅₈Cl₄N₂O₂P₄W₂·0.5CH₂Cl₂: C, 48.37; H, 3.89; Cl, 11.61; N, 1.83; P, 8.11. Found: C, 47.98; H, 3.81; Cl, 11.67; N, 1.76; P, 8.44%.

[WCl₂(Ph₂PMe)₂(CO)(NC₆H₄I-p)] 1p. para-Iodophenyl isocyanate **IIp** (0.10 g, 0.45 mmol) and [WCl₂(Ph₂PMe)₄] (0.43 g,

0.42 mmol) were placed in a Schlenk tube to which toluene (40 cm³) was added. After 3 h volatiles were removed under reduced pressure affording an oily purple solid. This was redissolved in diethyl ether (2 cm³) and light petroleum added to give pink complex **1p** (0.37 g, 91%) which was further washed with light petroleum. Crystals suitable for X-ray analysis were grown upon slow diffusion of methanol into a saturated dichloromethane solution. IR (CH₂Cl₂): 1967s cm⁻¹ (CO). ¹H NMR (CDCl₃): δ 7.73–7.31 (m, 20 H, Ph), 7.23 (d, J 8.0, 2 H, Ar), 6.13 (d, J 8.0, 2 H, Ar) and 2.32 (t, J 3.9 Hz, 6 H, Me). ³¹P NMR (CDCl₃): δ 2.80 (s, J$_{PW}$ 290 Hz). Mass spectrum (FAB): m/z 873 (M⁺ − CO). Calc. for C₃₃H₃₀Cl₂INOP₂W: C, 44.00; H, 3.33; N, 1.55. Found: C, 43.14; H, 3.22; N, 1.44%.

[WCl₂(Ph₂PMe)₂(CO)(NC₆H₄Br-p)] 1q. para-Bromophenyl isocyanate **IIq** (0.05 g, 0.25 mmol) and [WCl₂(Ph₂PMe)₄] (0.27 g, 0.26 mmol) were placed in a Schlenk tube to which toluene (30 cm³) was added. After 3 h volatiles were removed under reduced pressure affording an oily purple solid. This was redissolved in diethyl ether (2 cm³) and light petroleum added to give pink complex **1q** (0.19 g, 88%) which was further washed with light petroleum. IR (CH₂Cl₂): 1961s cm⁻¹ (CO). ¹H NMR (CDCl₃): δ 7.71–7.32 (m, 20 H, Ph), 7.02 (d, J 8.2, 2 H, Ar), 6.24 (d, J 8.2, 2 H, Ar) and 2.31 (t, J 4.0, 6 H, Me). ³¹P NMR (CDCl₃): δ 3.10 (s, J$_{PW}$ 290 Hz). Mass spectrum (FAB): m/z 825 (M⁺ − CO). Calc. for C₃₃H₃₀BrCl₂NOP₂W: C, 46.42; H, 3.52; N, 1.64. Found: C, 47.00; H, 3.50; N, 1.54%.

[WCl₂(Ph₂PMe)₂(CO)(p-NC₆H₄C≡CC₆H₅)] 1r. para-Phenylethynylphenyl isocyanate **IIr** (0.066 g, 0.30 mmol) and [WCl₂(Ph₂PMe)₄] (0.31 g, 0.30 mmol) were placed in a Schlenk tube to which toluene (30 cm³) was added. After 16 h, the green solution was filtered and volatiles were removed under reduced pressure affording a viscous green paste. This was redissolved in dichloromethane (2 cm³) and layered with methanol to give a green powder **1r** (0.15 g, 57%). Some decomposition occurred while standing in air and an analytically pure sample could not be obtained. IR (CH₂Cl₂): 1966s cm⁻¹ (CO). ¹H NMR (CDCl₃): δ 7.64–6.81 (m, 29 H, Ph + Ar) and 2.31 (t, J 4.0 Hz, 6 H, Me). ³¹P NMR (CDCl₃): δ 3.00 (s, J$_{PW}$ 292 Hz). Mass spectrum (FAB): m/z 845 (M⁺ − CO).

Attempted coupling of [WCl₂(Ph₂PMe)₂(CO)(NC₆H₄I-p)] 1p. Activated copper (0.011 g, 0.16 mmol) was added to a purple solution of complex **1p** (0.50 g, 0.06 mmol) in dmf (10 cm³). Upon heating to 110 °C the solution became red-orange and this was maintained for 15 min. After cooling to room temperature, grey CuI was removed via filtration to leave a red-brown solution from which volatiles were removed under reduced pressure to give an oily brown solid. A number of attempts were made to triturate this material from a range of solvents but with little success. Some material was soluble in dichloromethane and a mass spectrum (FAB) was obtained from this: m/z 1565, 1173, 1144 and 939.

Attempted coupling of complex 1p p-diiodobenzene. Activated copper (0.04 g, 0.61 mmol) was added to a pyridine solution (30 cm³) of complex **1p** (0.10 g, 0.019 mmol) and para-diiodobenzene (0.055 g, 0.01 mmol). After heating to 100 °C a red solution was formed, which after removal of CuI by filtration and removal of volatiles under reduced pressure, gave a red oil. Mass spectrum (FAB⁺): m/z 1634, 1435, 1246, 1046, 875, 855, 655 and 463.

X-Ray data collection and solution

Details of the crystal structure analyses of complexes **1a** and **1n** have been communicated previously.[9] For all structures a single crystal was mounted on a glass fibre and all geometric and intensity data were taken from this sample using an automated

Table 3 Crystallographic data for complexes **1a**, **1b**, **1g**, **1h**, **1n** and **1p**

	1a·C$_6$H$_5$Cl	1b	1g	1h·CH$_2$Cl$_2$	1n	1p
Formula	C$_{66}$H$_{61}$Cl$_5$N$_2$O$_2$-P$_4$W$_2$	C$_{61}$H$_{60}$Cl$_4$N$_2$O$_2$-P$_4$W$_2$	C$_{68}$H$_{64}$Cl$_4$N$_2$O$_4$-P$_4$W$_2$	C$_{65}$H$_{60}$Cl$_6$N$_2$O$_2$-P$_4$W$_2$	C$_{60}$H$_{56}$Cl$_4$N$_2$O$_2$-P$_4$W$_2$	C$_{33}$H$_{30}$Cl$_2$INOP$_2$W
Formula weight	1583.12	1486.49	1606.59	1605.43	1470.56	900.17
Crystal system	Triclinic	Monoclinic	Triclinic	Triclinic	Monoclinic	Orthorhombic
Space group	$P\bar{1}$	$P2_1/n$	$P\bar{1}$	$P\bar{1}$	$P2_1/a$	$Pcan$
a/Å	10.1257(12)	18.257(2)	11.3261(2)	11.865(3)	15.6810(28)	15.8427(13)
b/Å	11.5548(30)	8.855(2)	17.760(3)	16.051(5)	22.1749(50)	17.674(2)
c/Å	14.7543(32)	19.756(4)	18.226(3)	17.561(8)	17.0619(50)	24.198(5)
α/°	102.280(19)		99.320(12)	99.56(3)		
β/°	97.360(14)	107.130(13)	102.220(13)	97.73(3)	92.060(20)	
γ/°	91.770(16)		98.980(14)	98.21(2)		
V/Å^3	1669.5(6)	3052.0(10)	3466.2(10)	3221(2)	5929(2)	6776(2)
Z	1	2	2	2	4	8
μ(Mo-Kα)/cm^{-1}	38.53	40.89	36.09	39.61	42.91	46.00
Data measured	6204	556.7	8997	9406	11106	5904
Unique data used	4336	5382	8994	8871	7353	5883
No. parameters	338	343	510	715	667	370
R (all data)	0.039	0.031 (0.041)	0.53 (0.067)	0.080 (0.099)	0.041	0.045 (0.065)
R' (all data)	0.044	0.064 (0.069)	0.126 (0.136)	0.198 (0.209)	0.038	0.110 (0.126)

four-circle diffractometer (Nicolet R3mV) equipped with Mo-Kα radiation ($\lambda = 0.710\ 73$ Å) at 293 ± 2 K. The lattice parameters were identified by application of the automatic indexing routine of the diffractometer to the positions of a number of reflections taken from a rotation photograph and centred by the diffractometer. The ω–2θ or ω technique was used to measure reflections and three standard reflections (remeasured every 97 scans) showed no significant loss in intensity during data collection. The data were corrected for Lorenz-polarisation effects and empirically for absorption. The unique data with $I \geq n\sigma(I)$ ($n = 2$ or 3) were used to solve and refine the structures.

Structures were solved by either heavy atom methods (**1a**) or direct methods and developed by using alternating cycles of least-squares refinement and Fourier-difference synthesis. All non-hydrogen atoms were refined anisotropically. Hydrogens were placed in idealised positions (C–H 0.96 Å) and assigned a common isotropic thermal parameter ($U = 0.08$ Å^2). Final Fourier-difference maps were featureless and contained no peaks greater than 1.00 e Å^{-3}. Structure solution used either the SHELXTL[52] or SHELXTL PLUS[53] program packages on a microVax or IBM PC respectively. Crystallographic data are given in Table 3.

The structure of complex **1a** contains a molecule of chlorobenzene, which was refined only isotropically. A disorder in the solvent was successfully modelled by fixing the occupancy of the chloride [Cl(3)] to 50%. In **1b** the methyl group on the aryl ring was disordered over two sites [C(5) and C(5a)] the occupancies of each being fixed at 50%. In **1g** the carbons of the phenyl rings on phosphorus and the methoxy substituents on the central diaryl moiety were refined only isotropically, while a number of atoms [O(2), C(8), C(9), O(52), C(53), C(54), C(58)] were also disordered over two sites, occupancies being fixed at 50%. In **1h** a dichloromethane solvate molecule was refined only isotropically and a number of atoms [C(2), C(4), C(6), C(52), C(54), C(56)] were disordered over two sites with a fixed 50% occupancy.

CCDC reference number 186/1529.

Acknowledgements

References

1 M. D. Ward, *Chem. Soc. Rev.*, 1995, 121.
2 C. Creutz, *Prog. Inorg. Chem.*, 1983, **30**, 1.
3 W. Weng, T. Bartik and J. A. Gladysz, *Angew. Chem.*, *Int. Ed. Engl.*, 1994, **33**, 2199; M. Brady, W. Weng and J. A. Gladysz, *J. Chem. Soc.*, *Chem. Commun.*, 1994, 2655.
4 F. Coat and C. Lapinte, *Organometallics*, 1996, **15**, 477 and refs. therein.
5 W. A. Nugent and J. M. Mayer, *Metal–Ligand Multiple Bonds*, Wiley Interscience, New York, 1988.
6 T. P. Pollagi, S. J. Geib and M. D. Hopkins, *J. Am. Chem. Soc.*, 1994, **116**, 6051; H. A. Brison, T. P. Pollagi, T. C. Stoner, S. J. Geib and M. D. Hopkins, *Chem. Commun.*, 1997, 1263; B. E. Woodworth, P. S. White and J. S. Templeton, *J. Am. Chem. Soc.*, 1997, **119**, 828; B. E. Woodworth and J. L. Templeton, *J. Am. Chem. Soc.*, 1996, **118**, 7418; N. A. Ustynyuk, V. N. Vinogradova, V. G. Andrianov and Yu. T. Struchkov, *J. Organomet. Chem.*, 1984, **268**, 73; K.-Y. Shih, R. R. Schrock and J. Kempe, *J. Am. Chem. Soc.*, 1994, **116**, 8804; S. A. Krouse and R. R. Schrock, *J. Organomet. Chem.*, 1988, **335**, 257.
7 E. O. Fischer, D. Wittmann, D. Himmelreich and D. Neugebauer, *Angew. Chem.*, *Int. Ed. Engl.*, 1982, **21**, 454; G. Jia, W. F. Wu, R. C. Y. Yeung and H. P. Xia, *J. Organomet. Chem.*, 1997, **539**, 53; A. Rabier, N. Lugan, R. Mathieu and G. L. Geoffroy, *Organometallics*, 1994, **13**, 4676; N. Le Narvor, L. Toupet and C. J. Lapinte, *J. Am. Chem. Soc.*, 1995, **117**, 7129; H. Werner, T. Rappert and J. Wolf, *Isr. J. Chem.*, 1990, **30**, 377; D. Unseld, V. V. Krivykh, K. Heinze, F. Wild, G. Artus, H. Schmalle and H. Berke, *Organometallics*, 1999, **18**, 1525; R. S. Iyer and J. P. Selegue, *J. Am. Chem. Soc.*, 1987, **109**, 910; R. L. Beddoes, C. Bitcon, A. Ricalton and M. W. Whitley, *J. Organomet. Chem.*, 1989, **367**, C21; R. L. Beddoes, C. Bitcon, R. W. Grime, A. Ricalton and M. W. Whitley, *J. Chem. Soc.*, *Dalton Trans.*, 1995, 2873; M. I. Bruce, M. P. Cifuentes, M. R. Snow and R. T. Tiekink, *J. Organomet. Chem.*, 1989, **359**, 379; C. Löwe, H.-U. Hund and H. Berke, *J. Organomet. Chem.*, 1989, **372**, 295.
8 D. E. Wigley, *Prog. Inorg. Chem.*, 1994, **42**, 239.
9 G. Hogarth, R. L. Mallors and T. Norman, *J. Chem. Soc.*, *Chem. Commun.*, 1993, 1721.
10 M. Liang and E. A. Maatta, *Inorg. Chem.*, 1992, **31**, 953.
11 W. Clegg, R. J. Errington, D. C. R. Hockless, J. M. Kirk and C. Redshaw, *Polyhedron*, 1992, **11**, 381.
12 E. A. Maatta and D. D. Devore, *Angew. Chem.*, *Int. Ed. Engl.*, 1988, **27**, 569; J. L. Stark, A. L. Rheingold and E. A. Maatta, *J. Chem. Soc.*, *Chem. Commun.*, 1995, 1165.
13 W. Clegg, R. J. Errington, K. A. Fraser, S. A. Holmes and A. Schäfer, *J. Chem. Soc.*, *Chem. Commun.*, 1995, 455.
14 G. Hogarth, T. Norman and S. P. Redmond, *Polyhedron*, 1999, **18**, 1221.
15 E. A. Maatta and C. Kim, *Inorg. Chem.*, 1989, **28**, 624.

16 G. Hogarth and S. P. Redmond, unpublished results.
17 A. Antiñolo, F. Carrillo-Hermosilla, A. Otero, M. Fajardo, A. Garcés, P. Gómez-Sal, C. López-Mardomingo, A. Martín and C. Miranda, *J. Chem. Soc.*, *Dalton Trans.*, 1998, 59.
18 D. E. Wheeler, J.-F. Wu and E. A. Maatta, *Polyhedron*, 1998, **17**, 969.
19 R. K. Rosen, R. A. Anderson and N. M. Edelstein, *J. Am. Chem. Soc.*, 1990, **112**, 4588.
20 Y.-W. Ge, Y. Ye and P. R. Sharp, *J. Am. Chem. Soc.*, 1994, **116**, 8384.
21 P. R. Sharp, *Organometallics*, 1984, **3**, 1217.
22 (*a*) F.-M. Su, J. C. Bryan, S. Jang and J. M. Mayer, *Polyhedron*, 1989, **8**, 1261; (*b*) K. A. Hall and J. M. Mayer, *J. Am. Chem. Soc.*, 1992, **114**, 10402; (*c*) J. C. Bryan, S. J. Geib, A. L. Rheingold and J. M. Mayer, *J. Am. Chem. Soc.*, 1987, **109**, 2826.
23 A. P. Melissaris and M. H. Litt, *J. Org. Chem.*, 1994, **59**, 5918.
24 S. Takahashi, Y. Kuroyama, K. Sonogashira and N. Hagirara, *Synthesis*, 1974, 424.
25 H. Eckert and B. Forster, *Angew. Chem.*, *Int. Ed. Engl.*, 1987, **26**, 894.
26 H. Vittenet, *Bull. Soc. Chim. Fr.*, 1899, **3**, 956.
27 P. E. Fanta, *Synthesis*, 1974, 9; H. Tanaka, S. Sumida, N. Kobayashi, N. Komatsu and S. Torii, *Inorg. Chim. Acta*, 1994, **222**, 323.
28 M. P. Y. Yu, K.-K. Cheung and A. Mayr, *J. Chem. Soc.*, *Dalton Trans.*, 1998, 2373.
29 N. Kaltsoyannis and P. Mountford, *J. Chem. Soc.*, *Dalton Trans.*, 1999, 781 and refs. therein.
30 D. C. Bradley, M. B. Hursthouse, K. M. A. Malik, A. J. Nielson and R. L. Short, *J. Chem. Soc.*, *Dalton Trans.*, 1983, 2651.
31 T. Ziegler and A. Rauk, *Theor. Chim. Acta*, 1977, **46**, 1.
32 T. Ziegler and A. Rauk, *Inorg. Chem.*, 1979, **18**, 1558.
33 P. D. Lyne and D. M. P. Mingos, *J. Chem. Soc.*, *Dalton Trans.*, 1995, 1635.
34 H. Taube and D. E. Richardson, *Inorg. Chem.*, 1981, **20**, 1278.
35 J. E. McGrady, T. Lovell and R. Stranger, *Inorg. Chem.*, 1997, **36**, 3242.
36 J. C. Bryan and J. M. Mayer, *J. Am. Chem. Soc.*, 1990, **112**, 2298.
37 S. Cenini, M. Pizzotti, F. Porta and G. La Monica, *J. Organomet. Chem.*, 1975, **88**, 237.
38 J. Trotter, *Acta Crystallogr.*, 1961, **14**, 1135.
39 J. Almlö, *Chem. Phys.*, 1974, **6**, 135; O. Bastiansen and M. Traettenberg, *Tetrahedron*, 1962, **17**, 147.
40 J. L. Courtneidge, A. G. Davies, T. Clark and D. Wilhelm, *J. Chem. Soc.*, *Perkin Trans. 2*, 1984, 1197.
41 J. B. Flanagan, S. Margal, A. J. Bond and F. C. Anson, *J. Am. Chem. Soc.*, 1978, **100**, 4248.
42 S. L. W. McWhinnie, C. J. Jones, J. A. McCleverty, D. Collison and F. E. Mabbs, *J. Chem. Soc.*, *Chem. Commun.*, 1990, 940.
43 J. A. McCleverty, *Chem. Soc. Rev.*, 1983, **12**, 331; G. Denti, C. J. Jones, J. A. McCleverty, B. D. Neaves and S. J. Reynolds, *J. Chem. Soc.*, *Chem. Commun.*, 1983, 474.
44 N. AlObaidi, D. Clague, M. Chaudhury, C. J. Jones, J. A. McCleverty, J. C. Pearson and S. S. Salam, *J. Chem. Soc.*, *Dalton Trans.*, 1987, 1733; T. E. Berridge, F. S. McQuillan, H. Chen, T. A. Hamor and C. J. Jones, *Inorg. Chem.*, 1998, **37**, 4959.
45 J. A. Thomas, C. J. Jones, J. A. McCleverty, D. Collison, F. E. Mabbs, C. J. Harding and M. G. Hutchings, *J. Chem. Soc.*, *Chem. Commun.*, 1992, 1796.
46 R. J. H. Clark and D. G. Humphrey, *Inorg. Chem.*, 1996, **35**, 2053.
47 S. P. Best, S. A. Ciniawsky and D. G. Humphrey, *J. Chem. Soc.*, *Dalton Trans.*, 1996, 2945.
48 G. te Velde and E. J. Baerends, *J. Comput. Phys.*, 1992, **99**, 84.
49 ADF⟨2.3⟩, Department of Theoretical Chemistry, Vrije Universiteit, Amsterdam, 1997.
50 S. H. Vosko, L. Wilk and M. Nusair, *Can. J. Phys.*, 1980, **58**, 1200.
51 For details of both MOLDEN and ADFrom, the reader is directed to http://www.caos.kun.nl/~schaft/molden/molden.html
52 G. M. Sheldrick, SHELXTL, University of Göttingen, 1985.
53 G. M. Sheldrick, SHELXTL PLUS, Program package for structure solution and refinement, version 4.2, Siemens Analytical Instruments Inc., Madison, WI, 1990.

Paper 9/04001C